Universiteit Utrecht

Faculty of Geosciences

Master Thesis

Global spatial and temporal variation of biomass land-use emission factors

by

Iulia Pisca
4128974

Supervisor
Dr. Birka Wicke
MSc. Vassilis Daioglou
Second Reader
Dr. Floor van der Hilst

May 25th, 2015

Abstract

The global increase in biofuel demand is projected to be met at the expansion of bioenergy crops into natural vegetation areas. These land-use changes generate GHG emissions, which need to be factored in when assessing the bioenergy potential under sustainability targets. This study proposes the use of emission factors (EF) as the ratio of land-use change based emissions and the corresponding bioenergy potential, and emission factor supply curves (EFSC) which display the cumulative bioenenrgy potential at given EFs. Spatially specific global and regional EFs were derived for different EU RED emission reduction targets (ERT). Overall, bioenergy potential at current EU sustainability target (35% ERT) vary between 517EJ/yr and 182EJ/yr among the analyzed cases, with South America and Asia accounting for largest regional potentials. The associated EFSCs display generally steep slope suggesting that the marginal bioenergy potential decreases quickly to reach maximum potential, at the expense of the EFs. The main finding of this assessment is that bioenergy land-use EFs ($EF_{land-use}$) are highly spatially dependent, with baseline C stocks, soil C loss and bioenergy potentials, accounting as main contributor in its variability.

Contents

List of Figures

List of Tables

List of Abbreviations and Units

ABGC	Agriculture-bioenergy growth case
BGC	Bioenergy growth case
C	Carbon
CGE	Computable general equilibrium
CH_4	Methane
CO_2	Carbon dioxide
CO_2eq	Carbon dioxide equivalent
EJ	Exajoule; 1EJ=10^{18} Joule
EU	European Union
ERT	Emission Reduction Target
EF	Emission factor
$EF_{land-use}$	Land-use driven emission factor
EFSC	Emission factor supply curve
GHG	Greenhouse gas
GJ	Gigajoule; 1GJ=10^9 Joule
Gt	Giga tone
Ha	Hectare
IAM	Integrated assessment model
IPCC	International Panel for Climate Change
LUC	Land-use change
ILUC	Indirect land use change
Km	Kilometer
NVC	Natural vegetation case
N	Nitrogen
N_2O	Nitrous oxide
RED	Renewable Energy Directive
tC	Tone carbon
Yr	Year

1 Introduction

In 2012 energy related CO_2 emissions summed up to 32Gt CO_2, representing over 60% of global CO_2 emissions (IEA, 2014). It has been argued that part of these emissions can be mitigated in the future by expanding biomass use for bioenergy (Calvin et al., 2013; Daioglou et al., 2014; Rose et al., 2014). But bioenergy supply expansion triggers emissions of its own stemming from land use change (LUC) and intensified agricultural practices (Aalde et al., 2006). Much of the environmental stress of increased bioenergy in the global energy mix is related to agricultural land dynamics and the associated greenhouse gas (GHG) emissions (Searchinger et al., 2008; Fargione et al., 2008; Barona et al., 2010; Fritsche et al., 2010; Lapola et al., 2010; Popp et al., 2011; van der Hilst et al., 2014).

Increased bioenergy demand will put more pressure on food supply in competition for land. This can lead to an expansion of bienergy crops in areas deemed suitable on climatic and soil characteristics, with most pervasive examples involving the expansion into pasture land and forest. These market dynamics are argued to trigger land-use shifts which bare environmental concerns such as: GHG emissions (Kim et al., 2009; Hoefnagels et al., 2010), water cycles alterations (Berndes et al., 2003; Gerbens-Leenes et al., 2009), biodiversity disruptions (Sala et al., 2009; Wiens et al., 2011) and indirect land-use change (Fargione et al., 2008; Searchinger et al., 2008). Such issues render questinable the sustainability of bioenergy, and fueled a range of discussions in the academic community (Wicke et al., 2012; Milazzo et al., 2013), all leaning towards the conclusion that if not managed properly bioenergy cannot be competitive with fossil fuels in terms of its emissions.

The EU Renewable Energy Directive (RED)(European Commission, 2009) has established a set of bioenergy sustainability criteria under which emission reduction targets (ERT) are set in place. These ERTs are bioenergy GHG emissions savings targets, parallel to their fossil fuel alternatives. The current target is set at 35% emissions savings that bioenergy needs to deliver as compared to a counterfactual fossil fuel. This target is projected to increase to 50% in 2017, and 60% in 2018. This puts more pressure on full GHG emission inventories of bioenergy.

GHG emission accounting efforts of bioenergy (such as LCAs) are acknowledged to be faced with limitations brought about by the oversimplification of the applied methodologies, which lack sensitivity to a wide range of socio-economic drivers (Wicke et al., 2012). A number of socioeconomic and scientific modeling efforts, commonly referred to as integrated assessment models (IAM), have been able to accommodate the wide range of socio-economic interactions to assess different policy options (scenarios) for climate change mitigation. In this context, IAMs have been able to map LUC drivers and integrate them into spatially specific land-use outputs, yet there is little if any academic insight into how this plays out in determining spatially specific LUC driven bioenergy emissions.

Modeling efforts (Clarke et al., 2007; Popp et al., 2011; Klein et al., 2013; Stehfest et al., 2014) have facilitated the generation of spatially specific GHG fluxes in response to bioenergy demand, and related bioenergy potentials. Despite these IAMs returning spatially specific results, their outputs are mostly aggregated to global or macro-economic level (Nassar et al., 2011; Popp et al., 2014). There is little if any academic insight into how the spatially specificity of the data plays out in micro-trend analysis, relating the bioenergy potentials to their GHG emissions (temporal and spatial). These type of results can be further analyzed to gain insight into how bioenergy potential is related to GHG emissions and improve bioenergy crop allocation at different scales.

This assessment aims to compute spatially specific LUC driven CO_2 emissions of bioenergy and relate this spatially specific to bioenergy potential, in an attempt to offer a display of sustainable bioenergy potential at global level. The spatial aspect of the proposed methodology highlights the societal relevance of the research. Bioenergy has been under the scrutiny of sustainability criteria (Wicke et al., 2012; Milazzo et al., 2013)

because of the insufficient CO_2 emissions accounting. A vast part of the un-accounted CO_2 emissions are argued to stem from land-use changes associated with spatial allocation of the bioenergy crops (Fargione et al., 2008; Searchinger et al., 2008). As such, it is relevant to display and analyze the bioenergy potential and associated land-use emissions spatially specific.

The proposed assessment methodology makes use of spatially specific carbon stock, land-use and biomass potential maps, resulted from IMAGE 3.0 scenario runs. The carbon stocks are generated in 7 pools for two different bioenergy supply cases, which when compared to a baseline case without bioenergy, yield the corresponding CO_2 emissions. The concepts used by this methodology for mapping the emissions effect of bioenergy from land-use are the bioenergy *emission factor (EF) and the bioenergy emission factor supply curve (EFSC)*. The concept of bioenergy emission factor (EF) is defined here as, the ratio of CO_2 emissions generated per unit of energetic value created $[CO_{2eq}./GJ_{primarybiomass}]$. Ranking the mean annual cumulative bioenergy potential at given EFs generates the emission factor supply curve (EFSC).

Making use of the above stated concepts, this thesis aims to *assess the spatially specific bioenergy LUC EFs and highlight the relationship between increased bioenergy supply and marginal land-use GHG emissions.* Such an assessment is able to provide insights into the following intermediate aspects:

- From which biophysical processes do LUC emissions arise, and how do baseline assumptions affect them?
- What are the spatially specific primary EFs, and how do they vary across time steps?
- How do assumptions concerning time-span of bioenergy use affect the EF, under EU bioenergy sustainability criteria?
- How do marginal bioenergy EFSCs behave over time at global level, under the EU bioenergy sustainability criteria?
- Which regions and biomes are the most attractive for bioenergy production?

The following section provides and introspection into the existing studies surrounding this assessment, and highlights the research gap this assessment is proposing to address. The method and data input section, set-up the assessment's system boundary and describe the approach followed to answer the proposed research question. Ultimately, the description of the results alongside the discussion on data inputs, underlying assumptions and generated results, lead to the extraction of the thesis's conclusions.

2 Literature Review

A cornucopia of research has been devoted to assess, map and interpret the effects of land-use in relation to bioenergy production and consequent emissions (Kim et al., 2009; Verburg et al., 2009; Lapola et al., 2010; Popp et al., 2011; van der Hilst et al., 2013). Initial bioenergy studies focused on the assessment of bioenergy potential at different geographic scales, ranging from regional (van Dam et al., 2009) to global (Berndes et al., 2003; Hoogwijk et al., 2005; Smeets et al., 2007, Dornburg et al., 2010; Beringer et al., 2011). A critique to these studies is that they treated biomass potential at aggregate spatial scales, thus lacking sensitivity to the spatial distribution of the bioenergy potential. Despite the coarse resolution of the bioenergy assessments, these studies were quick to prompt concerns about the environmental impacts of increased bioenergy supplies (Berndes et al., 2003; Sala et al., 2009; Gerbens-Leenes et al., 2009; Kim et al., 2009; Hoefnagels et al., 2010). They identified that an increase in bioenergy potential is reckoned to trigger environmental perturbation, among which biodiversity loss, soil quality and water availability are the more worrisome.

Acknowledging these scientific handicaps triggered further scientific efforts into quantifying the environmental impacts associated with bioenergy potentials, while at the same time improving the spatial resolution of the bioenergy potential inventories. Biodiversity studies (Groom et al., 2008; Sala et al., 2009; Wiens et al., 2011) argue that a prevalent threat to biodiversity in relation to bioenergy expansion sets-off a domino effect which starts with land conversion, and continues with increased pollution, reduced perennial vegetation diversity and ends in biodiversity loss. Water availability (Berndes et al., 2003) and the water footprint of certain bioenergy forms (Gerbens-Leenes et al., 2009) adds to the list of environmental concerns rendering ever more questionable the sustainability bio-ethanol and bio-diesel. Alongside biodiversity loss and decrease in water availability, soil quality is one of the most pervasive environmental concerns (Kim et al., 2009; Hoefnagels et al., 2010).

Earlier academic discussions about the (un)sustainability of bioenergy crops such as palm oil or soy, point towards land-use change as the main driver. This occurs by converting carbon stock rich areas such as natural rainforest and peat swamp forest into pasture and agricultural land. The cumulative CO_2 emissions released from clearing natural vegetation via combustion and decomposition, as a reaction to land conversion, are commonly referred as the carbon debt of land use change (Fargione et al., 2007; Lamers and Juninger, 2013). The conversion of carbon stocks into CO_2 emissions is triggered by changes in both the above- and below-ground biomass. For perennial plants, the stocks are ephemeral which entails that the decay is balanced by re-growth "making the overall net carbon stock in biomass rather stable in the long term" (Aalde et al., 2006, p. 11). For trees and other woody materials, which over time accumulate carbon, it is relevant to account for the C fluxes which generate changes in the biomass pools (carbon reservoirs). The re-growth of woody biomass is challenged when dealing with the period of time it takes to accumulate the emitted carbon, as different woody biomass for bioenergy re-pays their carbon debt over different time spans.

The bioenergy sustainability criteria at aggregate levels have thus been challenged on environmental impacts and GHG emission accounting (Popp et al., 2011), all drawing to the same bleak conclusion that life-cycle assessment studies do not fully account for land-use driven GHG emission in relation to bioenergy production (Popp et al., 2011; Millazzo et al., 2013). It is argued that "biodiesels sustainability [for example] is usually compromised in case of land-use changes" (Millazzo et al., 2013) because the displacement of prior crop production most often leads to GHG balance shifts. This debate was adjoined by an earlier discussion about the induced indirect land-use effects of land-use displacement (Fargione et al., 2008; Searchinger et al., 2008). These issues emphasize on the need to include the corresponding emissions in the GHG balance calculations while at the same time improve the spatial resolution and extent of the study area (Fritsche et al., 2010; Wicke et al., 2012). The ILUC impacts on bioenergy added a new level of complexity to the GHG emission accounting methods which spurred a number of conspicuous unaccounted issues. Among the most notable ones are propagation effects of land displacement over time and space, but also spatially specific data characterization.

The complex land-use dynamics triggered related propagation effects of land displacement. Land-use change in a specific area, more than often, triggers changes elsewhere (within and/or outside boundaries). Spatially specific land-use displacements occur between different land classes, forcing for example agriculture to displace pasture while pasture advancing into forest to compensate for the takeover. One such study was performed by Barona et al. (2010) in the Brazilian Amazon finding that soy cultivations replace "previously deforested land and/or land previously under pasture" (p. 9) thus rendering deforestation merely a consequence of pasture expansion.

The uncertainties and inconsistencies among LUC GHG emission studies call for a more consistent conceptual frameworks. Several review studies have pointed out that despite applying similar methodologies to LUC GHG emission inventories, the results display wide ranges (Cherubini and Strmman, 2011; Vestegen et al., 2012; Wicke et al., 2012; DeCicco, 2013; Ahgren and DiLucia, 2014). Some of the bioenergy products displaying such large variations in GHG emissions are rapeseed biodiesel, soy biodiesel, corn ethanol and sugar cane ethanol. One of the most striking example in the series is that of corn-ethanol which evaluated across several studies ranged in emissions between 5-105 gCO_2 eq./MJ (Wicke et al., 2012). These uncertainties can arguably be sourced in methodological inconsistencies, ambiguities across definitions and different interpretations of the carbon payback period across land-use. The inconsistencies related to the methodological pathways such as temporal dynamics, can have different implications based on functional choices. Using a default 20 year carbon payback (IPCC, 2006) as compared to biomass specific carbon payback periods, can lead to disparities in the LUC GHG emissions, driven by endogenous land-use allocation priorities.

The LUC GHG emission inventories can arguably be deemed too simplistic in assumptions, drivers and spatial resolution, to generate robust estimates. The complexity of the interactions between different bioenergy drivers require an integrated approach to account for all the market feedbacks into the energy, economy, climate and land-use modules. A way to address the increasing size of complexity is through the use of computable general equilibrium (CGE) models which "provide a complete representation of national economies, including generation of factor income and expenditures" (Wicke et al., 2012, p. 88). This means that they use an elasticity factor to convert between land, labor and capital markets. The main advantage of using CGE to determine spatially specific LUC and associated GHG emissions is that they endogenously model land-use intensification and LUC.

A number of integrated assessment models (IAM) have been developed to spatially map the impact of large scale bioenergy crop production onto the emissions from land-use change. Among these IAMs, GCAM (Clarke et al., 2007), IMAGE (Stehfest et al., 2014) and ReMIND/MAgPIE (Popp et al., 2011; Klein et al., 2013) are the most cohesive in assumptions and method, and are thus relevant to refer to. The models are similar in their general approach to quantify the GHG emissions related to LUC in consequence to increased biomass supply, specifically, they all "contain both a dedicated energy system and land use module that interact with each other" (Popp et al., 2014, p. 496), thus covering for a wide range of drivers.

Apart from the general framework being similar across models, there are also notable differences among them. The main differences rest in the way they model biogeochemical and socio-economic processes, alongside the specificity of coverage and detail (ibid.). Specifically for the land-use module, an integrated part of the assessment, these models differ in the way they describe: (i) economic decisions associated with bioenergy supply, (ii) agricultural yield and how change is incorporated either endogenously (ReMIND) or exogenously (GCAM and IMAGE), (iii) land use based mitigation options, and (iv) carbon pools. These differences are strongly reflected in the results the models return. For example the cumulative global emissions from LUC through 2100 range considerably across models, from 11 to 89 Gt CO_2 eq..

Despite these IAMs returning spatially specific results, their outputs are mostly aggregated to global or

macro-level (Nassar et al., 2013; Popp et al., 2014). There is little if any academic insight into how the spatially specificity of the data plays out in micro-trend analysis relating the bioenergy potentials to their GHG emissions (temporal and spatial). This thesis aims to address the lack of spatially specific derived CO_2 emissions, and generate spatially specific EFs, and thus be able to map the relationship between bioenergy supply and marginal land use GHG emissions.

3 Method

This assessment seeks to explore biomass emission factors from land use change ($EF_{land-use}$) and how these may vary spatially and temporally. To estimate the spatio-temporal $EF_{land-use}$ from a set of baseline datasets requires the undertaking of a series of 3 intermediate steps: (a) carbon accounting, (b) emission accounting, and the (c) construction of emission factors. The assessment uses ArcGIS to display the maps, and Python to run the geo-processing of the data and plot all relevant results. The input maps are retrieved from the IMAGE model (Stehfest et al., 2014) and are described in the Data input section. The outputs of the study consist of (i) spatially explicit emission factor maps, (ii) emission supply curves. The maps and curves are capped at maximum $EF_{land-use}$ levels such that bioenergy can fulfill EU sustainability targets. Processed maps are generated at 10 year time steps, and 0.5x0.5 degrees grid cell resolution.

Bioenergy production from second-generation biomass has proven to offer energetic, environmental and economic advantages over first-generation sources (Hill, 2006; Melillo et al., 2009; Schmer et al, 2008; Dunn et al., 2013). Lignocellulosic biomass from perennial plants require few agricultural inputs, can be harvested multiple times per year and are less dependent on agricultural soil characteristics, thus returning lower CO_2 emissions as compared to fossil fuels (Melillo et al., 2009; Dunn et al., 2013). Such arguments aid the sustainability argument around bioenergy, and enforce the choice of lignocellulosic (grassy) biomass for this assessment. These include short-rotation tree plantations, switchgrass (*Panicus virgatum*), temperate short-rotation coppice trees (such as willow), tropical short-rotation coppice trees (such as eucalyptus) and Mischanthus (*Mischantus giganteus*) (Beringer et al., 2011).

The general aim of the proposed assessment methodology is to emphasize spatial and temporal change of lignocellulosic bioenergy $EF_{land-use}$. These EFs depend on a number of variables: (i) the carbon stock of the vegetation displaced, (ii) the baseline (also referred to as "counterfactual") changes of this carbon stock (i.e. forest carbon up-take or loss), and (iii) the energy content of the biomass growth. Thus, the analysis compares maps of carbon stocks under baseline and bioenergy cases. By carbon stocks, this study understands biomasss pools (reservoirs) which have the capacity to accumulate or release carbon over time. The carbon content maps in IMAGE are broken-down in 7 carbon pools corresponding to stems, branches, leaves, roots, soil litter, soil charcoal and soil hummus.

This assessment is based on the construction of three cases, one baseline case and two bioenergy cases. The baseline case, hereby referred to as the Natural Vegetation case (NVC), considers a potential regrowth of natural vegetation across all biomes taking into account the temporal consequences of climate change assuming no mitigation measures are taken throughout the projection period. The carbon stocks indicate a shift in biomes over time in line with most influential climate change natural impact studies available (Parmesan & Yohe, 2003; Bonan, 2008). Thus all results are relative to a situation where natural vegetation would prevail including areas that are considered agricultural lands.

The full bioenergy case, also referred to as the bioenergy growth case (BGC), assumes that bioenergy has the potential to be grown on all biophysically suitable grid cells. Consequently it ignores land-use for food production, which would lead to loss of carbon due to indirect land-use effects. In order to see how these results may change if agriculture is accounted for, a case where agriculture and bioenergy are both represented is constructed. This case is generically called the agriculture-bioenergy growth case (ABGC). It assumes that grassy biomass can be grown only after the food and fodder demand from agricultural land, as projected by IMAGE, is allocated.

An overview of the methodological flow is presented in *figure 1.*

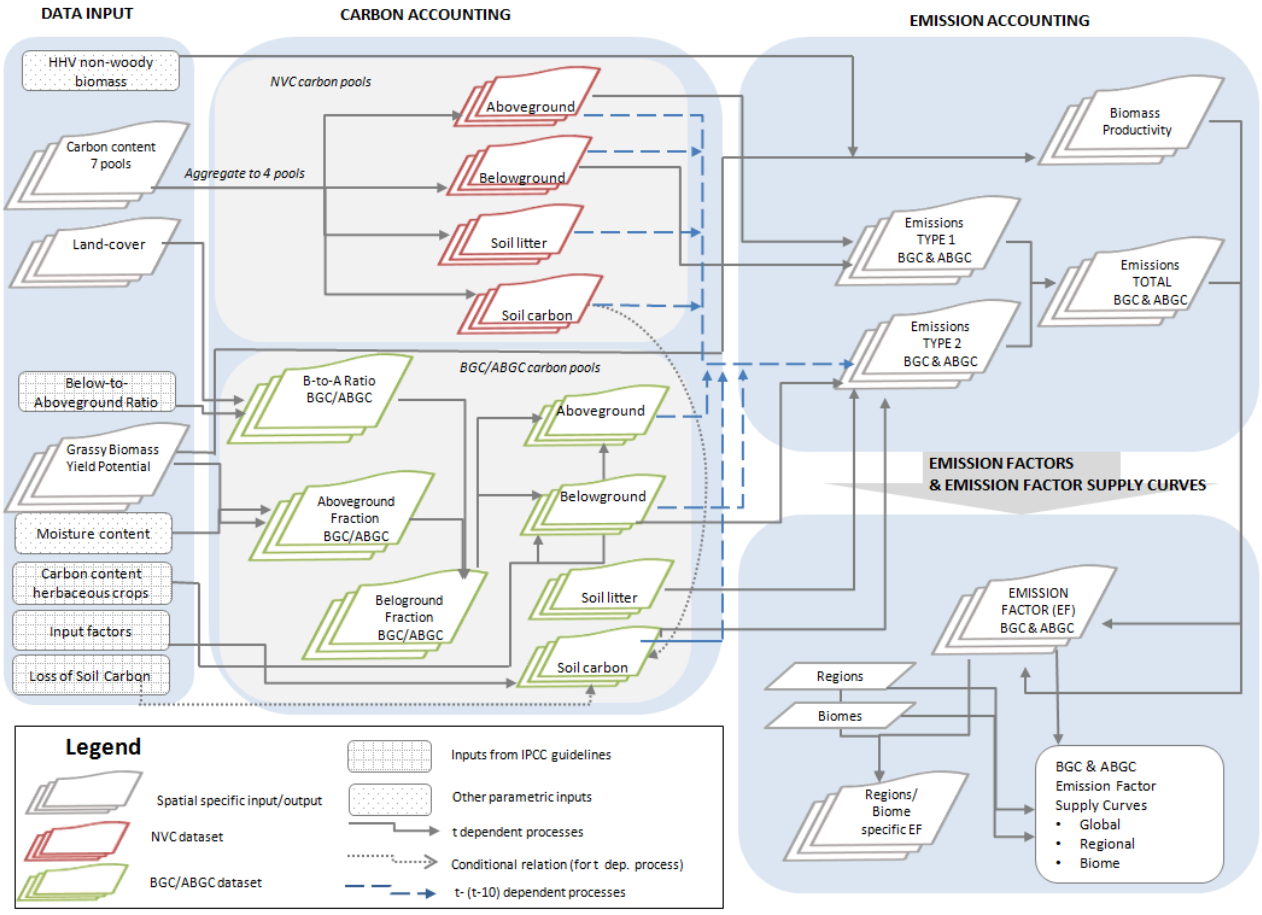

Figure 1: Methodological flow describing the three main steps for deriving the emission factors: (a) carbon accounting, (b) emission accounting and (c) construction of emission factor maps and curves

3.1 Carbon accounting

The carbon accounting step in the methodological flow consists of aggregating the IMAGE carbon pools to a set of 4 carbon pools for each of the cases. These pools are: above ground, below ground, soil litter and soil carbon Table 2. For the NVC, the spatially specific carbon pool data is available as an input from IMAGE.

Table 1: Carbon pool aggregation from the input dataset for the NVC

	Carbon pool input dataset	**Carbon pool output dataset**
1.	Stems	Above-ground
2.	Branches	
3.	Leaves	
4.	Roots	Below-ground
5.	Soil litter	Soil litter
7.	Soil charcoal	
6.	Soil humus	Soil carbon

For the bioenergy growth cases (BGC and ABGC) the carbon pools are derived using (i) spatially specific yield potentials for grassy biomass, (ii) below-to-above ground biomass ratio for different biomes, (iii) annual soil carbon loss estimates and (iv) grassy biomass specific parameters (moisture content, carbon content herbaceous crops). The parametrization and data is provided from IPCC guidelines and other sources, and detailed in the data input section.

3.1.1 Above ground pool

The *aboveground pool* [tC] is derived from the yield potential of the grassy crops in dry weight of carbon material as describe by eq.(1). The spatially specific computation is performed at each time step in the projection period. The change in land-use causes a change in the carbon pools, of which the above ground pool is subject to quickest shifts (Dunn et al., 2013). Because of the variation in the overall carbon stock, the change in land-use can lead either to a release or sequestration of carbon. This is especially relevant when converting high carbon stocks area, such as forests, into low carbon stock areas, such as agriculture.

$$\textit{Above ground carbon pool}_{BGC\ or\ ABGC_t} = NWYP_t * \frac{ha}{km^2} * (1 - mc) * CContent\ [\text{tC}] \tag{1}$$

$NWYP$ = Non Woody Biomass Yield Potential [t-biomass/ha]
mc = moisture content (10%)
$C\ Content$ = carbon content of herbaceous crops [tC/t-biomass (dry)] (0.47)
t = time step

3.1.2 Below ground pool

The computation of the belowground pool eq.(2) is based on the aboveground pool calculation with the addition of the below-to-above ground (BtA) biomass ratio. The BtA biomass ratio is used to generate BtA biomass ratio maps which display the BtA biomass ratio corresponding to land-cover class, using IPCC guideline values (table 4). In the calculation of the belowground biomass, the carbon content (C Content) is assumed to be the same as that of the aboveground pool.

$$\textit{Below ground carbon pool}_{BGC\ or\ ABGC_t} = \textit{Above ground carbon pool}_{BGC\ or\ ABGC_t} * BtA_t\ [\text{tC}] \qquad (2)$$

BtA = Below-to-Above ground biomass ratio [kg-below/kg-above]

3.1.3 Soil Carbon pool

The decision to plant grassy biomass at a certain year (t_{scen}) influences the value of the soil carbon pool as "land use and management have an [...] impact on organic carbon stocks" (IPCC Vol. 4, Chapter 2, p. 28). Land use change types, such as forest to cropland and grassland require the undertaking of a series of land management practices with strong impact on the soil organic carbon. IPCC reckons that these practices impact "plant production [...], direct additions of C in organic amendments, and the amount of carbon left after biomass removal, such as crop harvest" (p. 28). In addition, these changes in soil organic carbon levels can impact "erosion rates and subsequent loss of carbon from a site" (ibid).

For the years prior the plantation of grassy biomass, the value of the soil carbon pool is assumed the same as the soil carbon pool in NVC. For the 20 years period after the plantation of grassy biomass, the soil carbon pool undergoes both a loss and an accumulation. The linear loss rate is based on climate zone specific annual soil losses, subsequent to land-use conversion. The values used for annual carbon soil loss after land-use conversion are extracted from IPCC guidelines (Verchot et al., 2006), and are climate zone specific (Table 5). The sequestration is computed by means of land use, input and land management factors (Table 6) derived from IPCC guidelines. After the 20 years transition period, it is assumed that the soil loss soil carbon content remains constant whilst the carbon sequestration continues.

$$\textit{Soil Carbon pool}_{BGC\ or\ ABGC_t} = \begin{cases} \textit{Soil Carbon pool}_{NVC_t}\ [\text{tC}],\ \text{for} & t \leq t_{scen} \\ (\textit{Soil Carbon pool}_{NVC_t}) - (CarbonSoilLoss_t) * & \\ F_{textitLU} * F_{MG} * F_l\ [\text{tC}],\ \text{for}\ t_{scen} < t < t_{scen+20} & \\ (\textit{Soil Carbon pool}_{BGC\ or\ ABGC\ t_{scen+20}}) * & \\ F_{LU} * F_{MG} * F_l\ [\text{tC}],\ \text{for} & t \geq t_{scen+20} \end{cases}$$

t_{scen} = year of biomass planting
F_{LU} = Land-use factor
F_{MG} = Land management factor
F_I = Input factor

3.1.4 Soil Litter pool

The *soil litter* carbon pool accounts for the dead organic matter present for each vegetation type and land cover category. When converting a land cover to grassland, the IPCC indicates to account for a linear decline in soil litter over the coming 19 years after vegetation is cleared. There is a distinction to be made among land types when accounting for the soil litter pool. Not all land cover types accommodate a generous soil litter pool before conversion, and as such in the land use transition the IPCC proposes that this pool to be assumed zero (IPCC, 2006, p. 6.31). Other land cover types such as forest, agro-forest and wetlands have

significant soil litter pools which need to be accounted for in transition period after vegetation clearance (ibid.) according to eq.3, 4, 5.

$$Soil\ litter\ pool_{BGC\ or\ ABGC_t} = Soil\ litter_{NVC_{tscen}}/(t_{scen+20} - tscen)\ [\text{tC}] \tag{3}$$

$$Soil\ litter\ pool_{BGC\ or\ ABGC_{t_{scen+10}}} = Soil\ litter_{NVC_{tscen}}/\frac{1}{2}(t_{scen+20} - tscen)\ [\text{tC}] \tag{4}$$

$$Soil\ litter\ pool_{BGC\ or\ ABGC_{t_{scen+20}}} = 0 \tag{5}$$

$Soil_litter_{NVCtscen}$ = Carbon pool under the old landuse category [tC]

In a larger context, the accumulated carbon debt of bioenergy can be repaid over time. To take such aspects into account and for conservative reasons, this analysis assumes that biomass is to stay planted on the same plots for number of years, commonly referred to as biomass transition period. In the case of this assessment the transition period of biomass is assumed to be 20 years in line with the proposed IPCC guidelines for inventory methodologies (Aalde et al., 2006). After 20 years from the clearing of natural vegetation for grassy biomass planting, the bioenergy crops remain in place. The 20 year transition period is chosen "based on soil carbon pools typical time to equilibrium after land-use conversion" (p. 3.13). Figure 2 displays the change in carbon content across the three cases (NVC, BGC and ABGC).

3.2 Emission accounting

During land-use conversion from one type to another in the scope of growing biomass for bioenergy, CO_2 is emitted into the atmosphere. While these emissions are the aggregate of the carbon lost when vegetation is cleared, carbon stocks of natural vegetation may also change over time depending on biomass growth or loss. During land-use conversion, most of the CO_2 emissions happen instantaneously with the release of carbon from the above and belowground carbon pools. The remaining carbon accumulated in litter and soil carbon is released gradually over time "as soil carbon stocks [...] adjust to new equilibria" (Wise et al., 2015). Furthermore, carbon stock changes in the counterfactual should also be accounted for as forgone sequestration or emission.

The scope of the emission accounting step in the methodological flow is to generate spatially specific CO_2 emissions associated with land-use change. In line with the IPCC guidelines (Verchot et al., 2006), this assessment methodology takes into account 2 types of emissions: Emissions type 1 and Emissions type 2, once biomass is planted in t_{scen} and undergoes a 20 year transition period.

- **Emissions type 1** - The instantaneous emissions released in the atmosphere once natural vegetation is cleared, for grassy biomass plantation, are referred to as emissions type 1. They are based on the loss of carbon content of the present vegetation (above-ground, below-ground) in t_{scen} eq. (6).

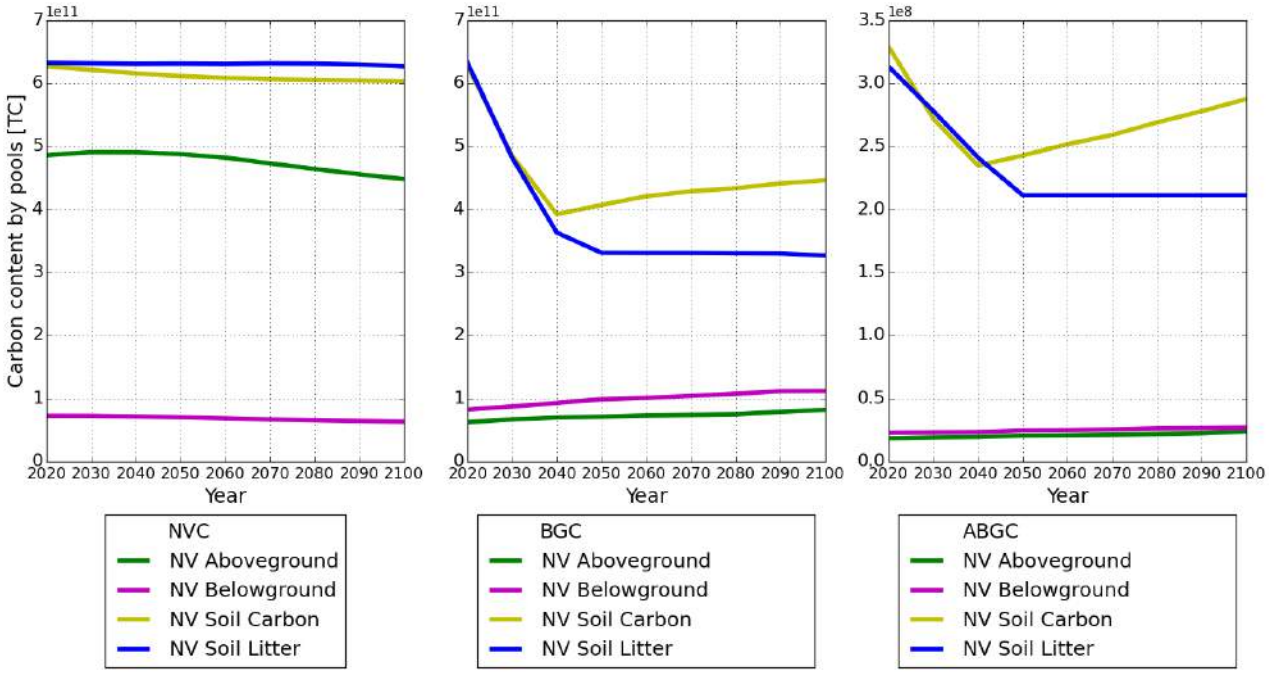

Figure 2: Land based C stocks by pool in the three cases. Parallel graphs of the carbon pool by content in the NVC (left), BGC (middle) and ABGC (right). Graphs are generated from input data under the above described assumptions. (left) The NVC displays a decrease in the above ground and soil carbon pools after 2040 linked to the impacts of climate change across natural systems. (middle) The BGC marginally accumulates carbon in the above and below ground pools till 2100, though these are lower than in the NVC. The soil carbon pool decreases rapidly in the transition period because of rapid soil erosion associated with land conversion, but faces a meager increase as a consequence of C accumulation in the soil horizon. (right) The change in C stock is emulated in the ABGC, but at lower C stock levels because agricultural lands are exempted form the analysis.

$$Emissions\ type\ 1_t = (Above\ ground_{NVC_t} + Below\ ground_{NVC_t} * \frac{44}{12}\ [\text{kg } CO_2] \tag{6}$$

- **Emissions type 2** - Over the coming t_{scen} -1 years from grassy biomass planting, emissions will continue to be diffused into the atmosphere emanating from the belowground, soil litter and soil carbon polls which diffuse their carbon content at a slower pace. Changes in the carbon content (emission or sequestration) over the coming t_{scen} -1 years, in the baseline, are also accounted for. These emissions are referred to as emissions type 2, and represent the baseline changes in carbon content between the NVC and the BGC/ABGC eg. (7-13).

  For example in the NVC, the above-ground carbon pool may have sequestered carbon over time if it were to continue being planted. As the natural vegetation is cleared, the avoided carbon sequestration of the natural vegetation growth needs to be accounted for as an emission against the BGC /ABGC eq.(7-13).

One of the assumptions involved in the calculation of emissions type 2 is that the above ground biomass in the BGC/ABGC is harvested annually to be used as bioenergy, hence the carbon accumulated over the year is burned quickly. This leaves only the belowground, soil litter and the soil carbon pools sequestering carbon over time.

$$Carbon\ stocks_{BGC\ or\ ABGC_t} =$$

$$(Below\ ground_{BGC\ or\ ABGC_t} + Soil\ Carbon_{BGC\ or\ ABGC_t} + Soil\ litter_{BGC\ or\ ABGC_t}) \tag{7}$$

$$Carbon\ stocks_{BGC\ or\ ABGC_{t\text{-}10}} =$$

$$(Below\ ground_{BGC\ or\ ABGC_{t\text{-}10}} + Soil\ Carbon_{BGC\ or\ ABGC_{t\text{-}10}} + Soil\ litter_{BGC\ or\ ABGC_{t\text{-}10}}) \tag{8}$$

$$Carbon\ stocks_{NVC_t} =$$

$$(Above\ ground_{NVC_t} + Belowground_{NVC_t} + Soil\ Carbon_{NVC_t} + Soil\ litter_{NVC_t}) \tag{9}$$

$$Carbon\ stocks_{NVC_{t\text{-}10}} =$$

$$(Above\ ground_{NVC_{t\text{-}10}} + Belowground_{NVC_{t\text{-}10}} + Soil\ Carbon_{NVC_{t\text{-}10}} + Soil\ litter_{NVC_{t\text{-}10}}) \tag{10}$$

$$\triangle Carbon\ stocks_{NVC} = Carbon\ stocks_{NVC_t} - Carbon\ stocks_{NVC_{t\text{-}10}} \tag{11}$$

$$\triangle Carbon\ stocks_{BGC\ or\ ABGC} = Carbon\ stocks_{BGC\ or\ ABGC_t} - Carbon\ stocks_{BGC\ or\ ABGC_{t\text{-}10}} \tag{12}$$

$$Emissions\ type\ 2_t = (\triangle Carbon\ stocks_{NVC_t} - \triangle Carbon\ stocks_{BGC\ or\ ABGC_t}) * \frac{44}{12}\ [\text{kg } CO_2] \tag{13}$$

The typical pattern of emissions from land-cover change due to growth of biomass displays as an initial pulse from net change in carbon balance (type 1) followed by a long tail of lagged changes in pools such as soil carbon and baseline vegetation changes (type 2).

The integral of the emissions over the transition period display the cumulative CO_2 emissions associated with the land use conversion for bioenergy eq.(14). The cumulative emissions are computed for the two cases (BGC and ABGC), and displayed spatially specific (in a map format).

$$Cumulative\ emissions(CE)_{t_{scen+20}} = \int_{t_{scen+20}}^{t_{scen}} (Emissions\ type\ 1 + Emissions\ type\ 2)\ [\text{kg } CO_2] \tag{14}$$

The grassy bioenergy emissions are linked to the bioenergy potential, which is why it is relevant to compute the potential both spatially specific and aggregate potentials, until $t_{scen+20}$. The cumulative biomass

production, assessed in $GJ_{primary}$ per grid cell, is a function of potential grassy biomass yield and HHV for non-woody energy crops eq. (15) . The value of the HHV for non-woody energy crops used in this assessment is 16.5 MJ/kg, and is extracted from the ECN-Phyllis database, corresponding to switchgrass and Miscanthus.

$$\textit{Cumulative grassy biomass production (CEP)}_{t_{scen+20}} = \int_{t_{scen}}^{t_{scen+20}} (\textit{Biomass yield} * HHV_{non-woodyenergycrops} * \frac{ha}{km^2} * Area) \tag{15}$$

$$\left[\frac{GJ_{primary\ biomass}}{grid\ cell}\right] = \left[\frac{10^3 kg}{ha}\right] * \left[\frac{MJ}{kg}\right] * \left[\frac{ha}{km^2}\right] * \left[\frac{km^2}{grid\ cell}\right]$$

3.3 Emission factors

Carbon balance of bioenergy is often expressed as the ratio of CO_2 emissions generated per unit of energetic value, commonly referred to as the emission factor (EF) of bioenergy (Lamers and Juninger, 2013). These EFs can be put into perspective globally by means of *emission factor maps*. This spatially specific approach, emphasizing the trade-offs between temporal LUC emissions incidental to bioenergy potential, is necessary for two reasons. First makes it possible for land-cover change and the consequent CO_2 emissions from bioenergy to be fully accounted at grid cell level over time. As such, this assessment overcomes averaging limitations and regional isolation of emission impacts. Second, at regional levels, EF maps can provide categorical differences between analyzed cases (BGC and ABGC).

The emission factor of biomass planted at t_{scen} for a transition period of 20 years is calculated according to eq. (16) and represents the land-use EF of bioenergy ($EF_{landuse}$). This type of analysis has an implication on the choice of t_{scen} and the transition period of bioenergy.

$$\textit{Emission Factor}(EF_{20}) = \frac{CE_{t_{scen+20}}}{CBP_{t_{scen+20}}} \frac{[kg_{CO_2}]}{GJ} \tag{16}$$

The relevance of computing $EF_{landuse}$ is threefold. First, by performing a spatially specific assessment the results provide information of the performance of each individual grid cell, giving the possibility to extract EF information about specific regions and biomes. Second, the methodology allows to assess the performance of spatially specific and aggregate $EF_{landuse}$ at different biomass planting years. For example, the base set of results are constructed on the assumption that biomass is planted in 2020, but this can be adjusted to 2010 or 2030. Third, the bioenergy transition period is assumed 20 years but this default transition period can be exercised on shorter and longer intervals. One interesting alternative is 30 year stationary effect, prevalent in US based studies (Schmer et al., 2007; Dunn et al., 2013).

The spatially specific $EF_{land-use}$ alongside the bioenergy potential can be used to generate emission factor supply curves (EFSC) which display the cumulative mean annual bioenergy potential within a given $EF_{land-use}$. The EFSC are computed for both the BGC and the ABGC. The difference between the two cases consists in the fact that the ABGC will have far less grid cells available for bioenergy, meaning that the ABGC EFSC has a lower cumulative bioenergy potential. This does not need to hold true across all

world regions. Filters for specific regions and biomes around the globe can indicate at specific $EF_{land-use}$ threshold levels, the cumulative suitability for bioenergy growth. Spatially specific, this type of information can point to clusters of bioenergy suitable grid cells.

This analysis considers as base case the situation of 2020 as t_{scen} and 20 years transition period. Variations of t_{scen} and transition period, in the construction of the EFSC, are performed for analysis.

3.4 Thresholds for sustainable bioenergy land-use EFs

Under the EU Renewable Energy Directive (RED)(EU Commission, 2009) the renewable energy targets require that in order for biofuels to displace sustainably fossil fuels, they need to provide GHG emission savings, compared to the their fossil fuel alternatives. The current target is set at 35% GHG emissions saving, but this is to increase to 50% in 2017, and 60% in 2018 (ibid.).

The purpose of this step of the analysis is to assess what are the thresholds for $EF_{land-use}$ of bioenergy, such that bioenergy can fulfill the EU Renewable Energy Directive sustainability criteria (Table x in the data input section). A first step is to include the EFs of the other processes ($EF_{bioenergy\ porcesses}$) involved in the bioenergy production such as cultivation, transport and processing, from the JRC inventory (Edwards et al., 2014). As gasoline and bioethanol can substitute each other in the transportation sector, gasoline is reckoned to be, in this second step, the fossil fuel alternative. The LCA EF of gasoline used in this assessment is 87.1 kg_{CO2eq}/GJ_{fuel} (ibid.). In a third step, the EU RED sustainability EF ($EF_{sustainability\ target}$) are calculated, added to the $EF_{bioenergy\ porcesses}$, and subtracted from the $EF_{gasoline}$. The resulting estimates represent the upper thresholds for $EF_{land-use}$ for EU biofuel sustainability standards. To round-up the analysis, the spatially specific $EF_{land-use}$ are capped (table x), in the EF maps and the EFSCs, to contextualize the results in the EU RED sustainability guidelines. The capped EF maps indicate the spatial distribution of the sustainable bioenergy, while the EFSC provide an indication of the order of magnitude of the sustainable bioenergy potential.

Table 2: Maximum $EF_{land-use}$ in line with EU RED sustainability targets

EU RED sustainability target[a]	**35**%	**50**%	**60**%
Maximum $EF_{land-use}$ (primary biomass) $[kgCO_{2eq}/GJ_{primary}]$	85	52	30

[a]expressed as % of the GHG emission savings compared to the their fossil fuel alternatives

4 Data input

This assessment is constructed on the inputs listed in table 3, and mostly sourced from IMAGE and the IPCC guidelines.

Table 3: List of assessment inputs

Input	**Type**	**Unit**
IMAGE inputs		
Land use maps natural vegetation[a]	Land-cover raster	Land use classes
Land use maps bioenergy growth cases	Land-cover raster	Land use classes
C content maps	Raster	tC/km^2
Grassy crops yield potential map	Raster	$t_{(wetbased)}$/ha
Area map	Raster	Km^2
Region map[b]	Raster	regions
IPCC inputs		
Below-to-Aboveground Ratio	ratio	$tC_{belowground}/tC_{aboveground}$
Soil Loss	ratio	[tC/ha/year]
Input factors	factor	-
OTHER inputs		
Herbaceous crops moisture content[c]	value	Mass water/mass biomass
Carbon content[d]	value	tC/t-biomass (dry)
EF bienergy processes[e]	values	$kgCO_{2eq}/GJ_{EtOH}$

[a] Appendix 1

[b] Appendix 2

[c] Value wet to dry grassy biomass of 0.1 (ECN Phyllis, 2014)

[d] Value 0.47 tC/t-biomass (dry) extracted from the IPCC guidelines for herbaceous crops (Verchot et al., 2006)

[e] EU Joint Research Center (JRC), Well-to-wheel analysis (Edwards et al., 2014)

4.1 IMAGE inputs

IMAGE is an IAM of the global environmental change which takes into account the interactions between the human and the Earth system. IMAGE is built on a number of exogenous assumptions (drivers) which shape the direction and rate of change in key variables and results. These drivers are: natural resource availability, technological development, economy, demographics, policy and governance, and culture and lifestyle. The spatial projections of the IMAGE 3.0 model assess the biophysical limits of scenario expansion (Stehfest et al., 2014). Within the scope of this assessment, the most relevant spatially specific outputs are: (i) land use - natural vegetation map, (ii) land-use bioenergy growth case, (iii) carbon content maps, and (iv) yield potential maps for grassy crops.

The temporal resolution of the maps is 10 year time steps in the interval 2000 to 2100, and the spatial resolution of the maps is 0.5x0.5 degrees. This means that for each of the cases, the bioenergy and GHG emission maps are generated at every 10 year time intervals and return maps consisting of over 60.000 grid cells.

(i) Land use - natural vegetation and **(ii) Land use bioenergy growth case** - a set of raster files generated by IMAGE which pin down the type of potential vegetation at each grid cell. In IMAGE 3.0 (Stehfest et al., 2014) land use allocation causes LUC and subsequently triggers a set of GHG fluxes between the land cover, soil and atmosphere. In order to map these "complex dynamics of the terrestrial biosphere"

(p. 175) IMAGE uses the LPJmL model (Lund-Potsdam-Jena model with managed land) (Sitch et al., 2003). The LPJmL is one of the most extensively evaluated dynamic global vegetation models (ibid.) which in the scope of this assessment uses the carbon dynamics outputs in the form of a global map with 0.5x0.5 degrees resolution accounting at each grid cell for the content of the different carbon pools (ibid.).

IMAGE applies a number of rules in the land-use allocation, which assess where the different classes will be located. These rules iterated on a yearly basis and are driven by a suitability assessment. The suitability function factors in potential yield and terrain slope index. The suitability function is thus concerned with the individual cell productivity rather than emission dynamics (Stehfest et al., 2014).

(iii) Carbon content maps - for different carbon pools are a set of raster files generated by IMAGE and accounting for the carbon content at 7 different biomass pools figure 3.

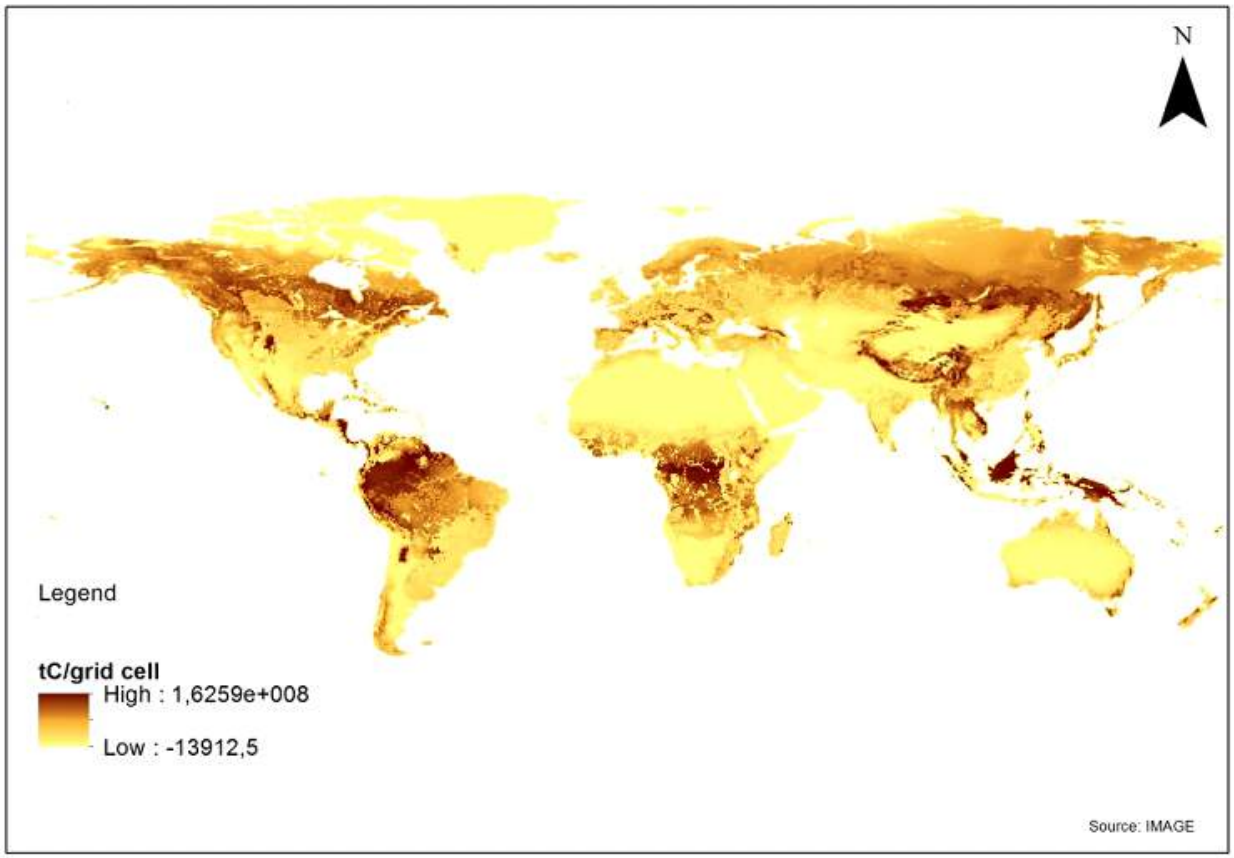

Figure 3: Aggregate carbon pools - natural vegetation

(iv) Potential yield of non-woody (grassy) crops represents a set of raster maps which indicate the potential yield (wet based) in t/ha at grid cell level. IMAGE assumes an average autonomous yield increase of 1%/year, differentiated by region (Stehfest et al., 2014, p. 189).

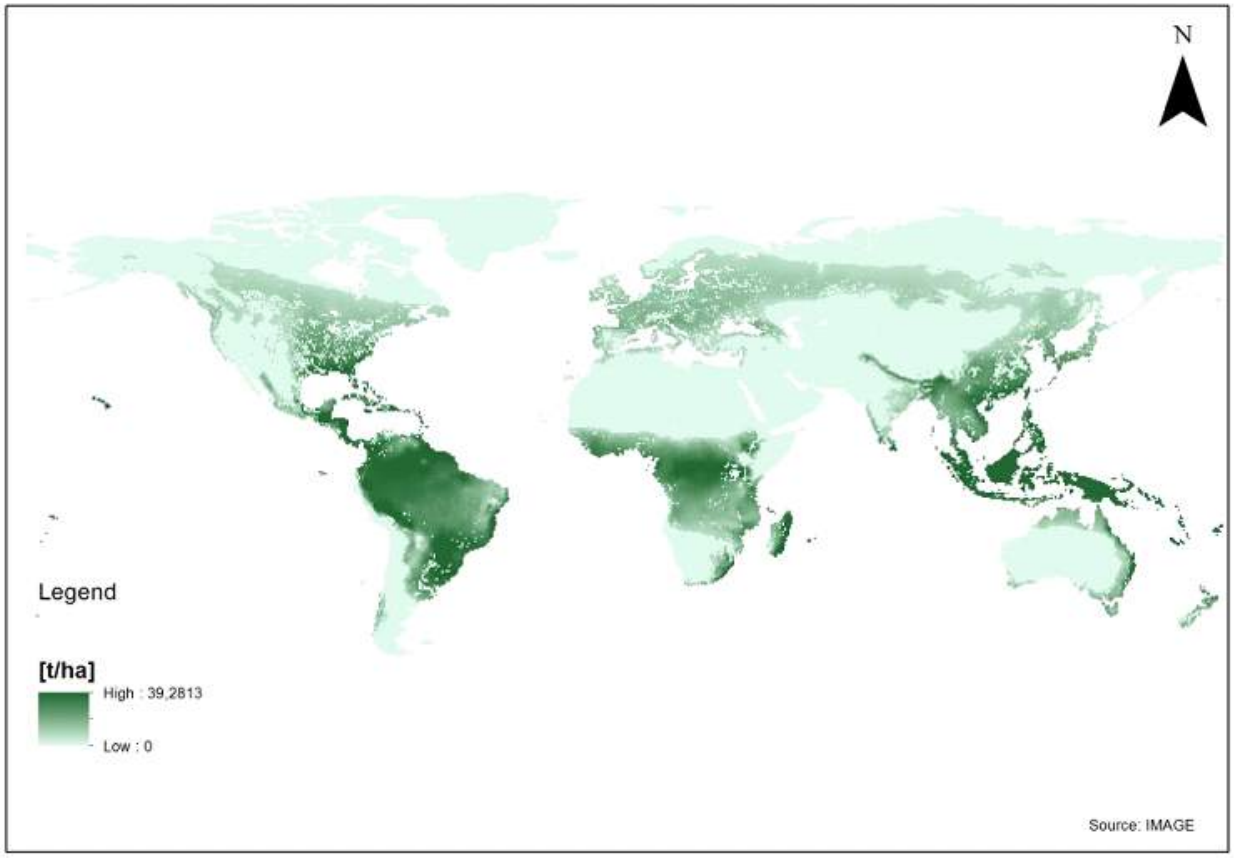

Figure 4: Yield potential for non woody biomass in 2020

4.2 IPCC inputs

A number of specific parameters used to derive the C content of the C pools in the bioenergy case, based on he IPCC guidelines. They are: below-to-aboveground ratio (table 4), the annual soil C loss (table 5) and the bioenergy input factors (table 6).

Table 4: The below-to-above ground biomass ratio, for the major grassland ecosystems of the world (IPCC, 2006, vol. 4, ch. 6, table 6.1)

Vegetation Type	**Approximate climate zone**	**Below-to-Above ground Ratio**
Steppe/tundra/prairie grassland	Boreal - dry and wet Cold Temperate wet Warm Temperate - wet	4.0
Semi-arid grassland	Cold Temperate dry Warm Temperate dry Tropical - dry	2.8
Sub-tropical/tropical grassland	Tropical Moist and wet	1.6
Woodland/savannah	Savannah	0.5
Shrubland	Shrubland	2.8
Other vegetation types*		2.0

*own estimate for remaining vegetation types

Table 5: Annual soil carbon loss as a result to land-use change for biomass planting (IPCC, 2006, vol. 4, ch. 6, table 6.3)

IPCC climatic zone	**Soil loss** [tC/ha per year]
Boreal /Cold Temperate	0.25
Warm Temperate	2.5
Tropical/Subtropical	5.0

Table 6: Input factors for land-use conversion (IPCC,2006, vol. 4, ch. 5, table 5.5)

Climatic zone	**Input factor** (F_I)	**Land-use factor** (F_{LU})	**Management factor** (F_{MG})
Temperate dry	1[2]	0.93	1.10
Temperate wet	1[2]	0.82	1.15
Tropical dry	1[2]	0.93	1.17
Tropical wet	1[2]	0.82	1.22
Tropical mountain	1[2]	0.88	1.16

4.3 Other inputs

Table 7 provides the inputs for the derivation of the $EF_{land-use}$.

Table 7: Input data for the $EF_{land-use}$ calculation

Parameter		**Unit**	**Value**	**Source**
$EF_{\textit{bioenergy porcesses}}$[a]	Cultivation[b]	$kgCO_{2eq}/GJ_{EtOH}$	6.3	Edwards et al. (2014 - Appendix 4)
	Processing[c]	$kgCO_{2eq}/GJ_{EtOH}$	14.0	
	Transport[d]	$kgCO_{2eq}/GJ_{EtOH}$	2.5	
	Combustion	$kgCO_{2eq}/GJ_{EtOH}$	74.1	
	of which renewable	$kgCO_{2eq}/GJ_{EtOH}$	-74.1	
	Total		**22.8**	
$EF_{\textit{sustainability target}}$[e]	2010 - (-35% target)	$kgCO_{2eq}/GJ_{EtOH}$	30.5	EU Commission (2009)
	2015 - (-50% target)	$kgCO_{2eq}/GJ_{EtOH}$	43.6	
	2020 - (-60% target)	$kgCO_{2eq}/GJ_{EtOH}$	52.3	
Upper $EF_{land-use}$**(ethanol)**	current - (-35%)	$kgCO_{2eq}/GJ_{EtOH}$	33.8	Own calculations[f]
	2017 - (-50%)	$kgCO_{2eq}/GJ_{EtOH}$	20.7	
	2018 - (-60%)	$kgCO_{2eq}/GJ_{EtOH}$	12.0	
Conversion efficiency (η)	40% [g]			
Upper $EF_{land-use}$ **(primary biomass)**	current - (-35%)	$kgCO_{2eq}/GJ_{primary}$	84.5	Own calculations [h]
	2017 - (-50%)	$kgCO_{2eq}/GJ_{primary}$	51.8	
	2018 - (-60%)	$kgCO_{2eq}/GJ_{primary}$	30.0	

[*] EF - Emission factor

[a] the emission factor of the bioenergy processes correspond to waste wood to ethanol production. It is assumed that the emission factors of waste wood for ethanol production are the closest in the LCA to those of second generation lignocellulosic crops for bioenergy production.

[b] the cultivation includes fertilization, diesel based agricultural management inputs and storage of primary bioenergy.

[c] processing refers to the conversion from primary biomass to ethanol with diesel inputs. The JRC inventory (Edwards et al., 2014) assumes 34% conversion efficiency for this process, and accounts for credit for surplus electricity based on biomass fuelled power station at 32% conversion efficiency.

[d] transportation includes three transport segments: (i) primary biomass transport from source to conversion facility (average 150km). (ii) ethanol transport to distribution center (average 150km), (iii) ethanol transport to retail sites

[e] this study assumes that the energetic conversion between ethanol and gasoline is 1:1

[f] the maximum EF land-use - ethanol is calculated as:

$EF_{landuse-ethanol}[kgCO_{2eq}/GJ] =$

$EF_{\textit{fossil fuel alternative}}[kgCO_{2eq}/GJ]$-$EF_{\textit{bioenergy porcesses}}[kgCO_{2eq}/GJ]$-$EF_{\textit{sustainability target}}[kgCO_{2eq}/GJ]$;

with energetic conversion between ethanol to gasoline as 1:1

[g] because the spatially specific results are generated in primary energy, there is a need to convert from $kgCO_{2eq}/GJ_{EtOH}$ to $kgCO_{2eq}/GJ_{primary}$. Assumed conversion efficiency = 40%. The biochemical feedstock to fuel conversion efficiency ranges in practice from 37% (EPA, 2010) to 44% (Bain, 2007) for second generation biofuels from lignocellulosic.

[h] the maximum EF land-use primary biomass is calculated as:

$EF_{landuse-primary}[kgCO_{2eq}/GJ] = EF_{landuse-ethanol}[kgCO_{2eq}/GJ]/\eta$

5 Results

5.1 Base case

5.1.1 CO_2 emissions

The land use change CO_2 emissions for bioenergy growth are presented in figure 5. The type 1 emissions resulting from the clearance of natural vegetation for planting bioenergy crops, for both analyzed cases, return the same pattern. On the time profile, the emissions spike in the year the switch is made from natural vegetation to grassy crops as the vegetative C stocks are cleared. Once the instantaneous emissions are released, the type 2 emissions, resulting from the gradual release of CO_2 as a consequence remainder organic material decay, as well as baseline changes in carbon stocks, are diffused gradually over the transition period.

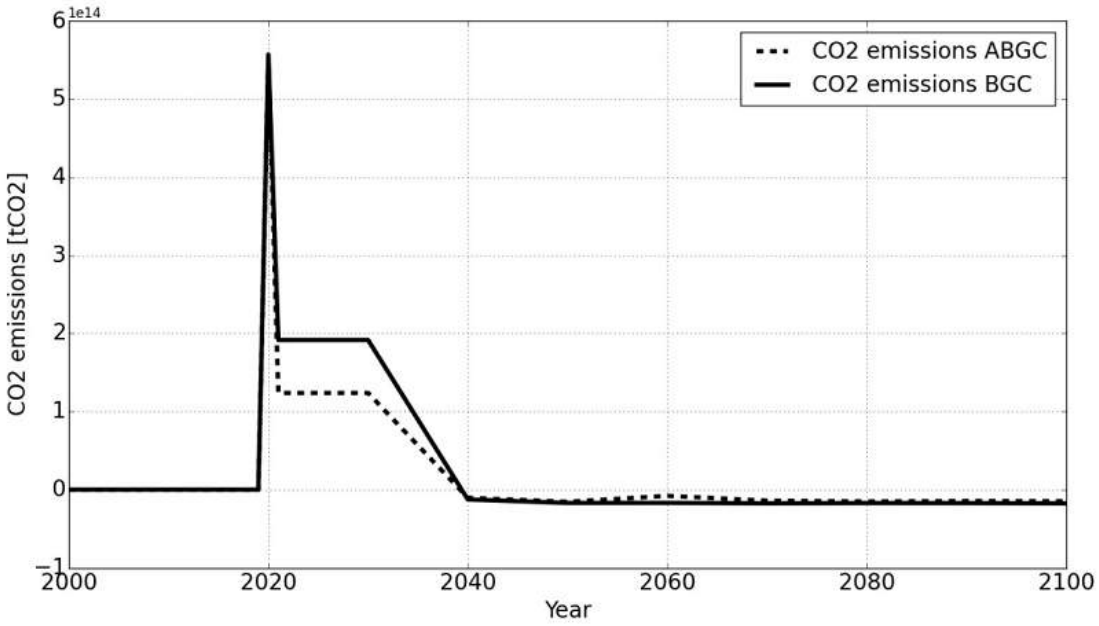

Figure 5: Time path of land-use change driven CO_2 emissions in the BGC and the ABGC

5.1.2 Emission factors

The $EF_{land-use}$, constructed from the CO_2 emission data and the bioenergy potential, is mostly relevant in a spatially specific analysis (figure 6). In line with the EU RED biofuels sustainability criteria, the upper $EF_{land-use}$ are displayed globally according to the pre-calculated thresholds.

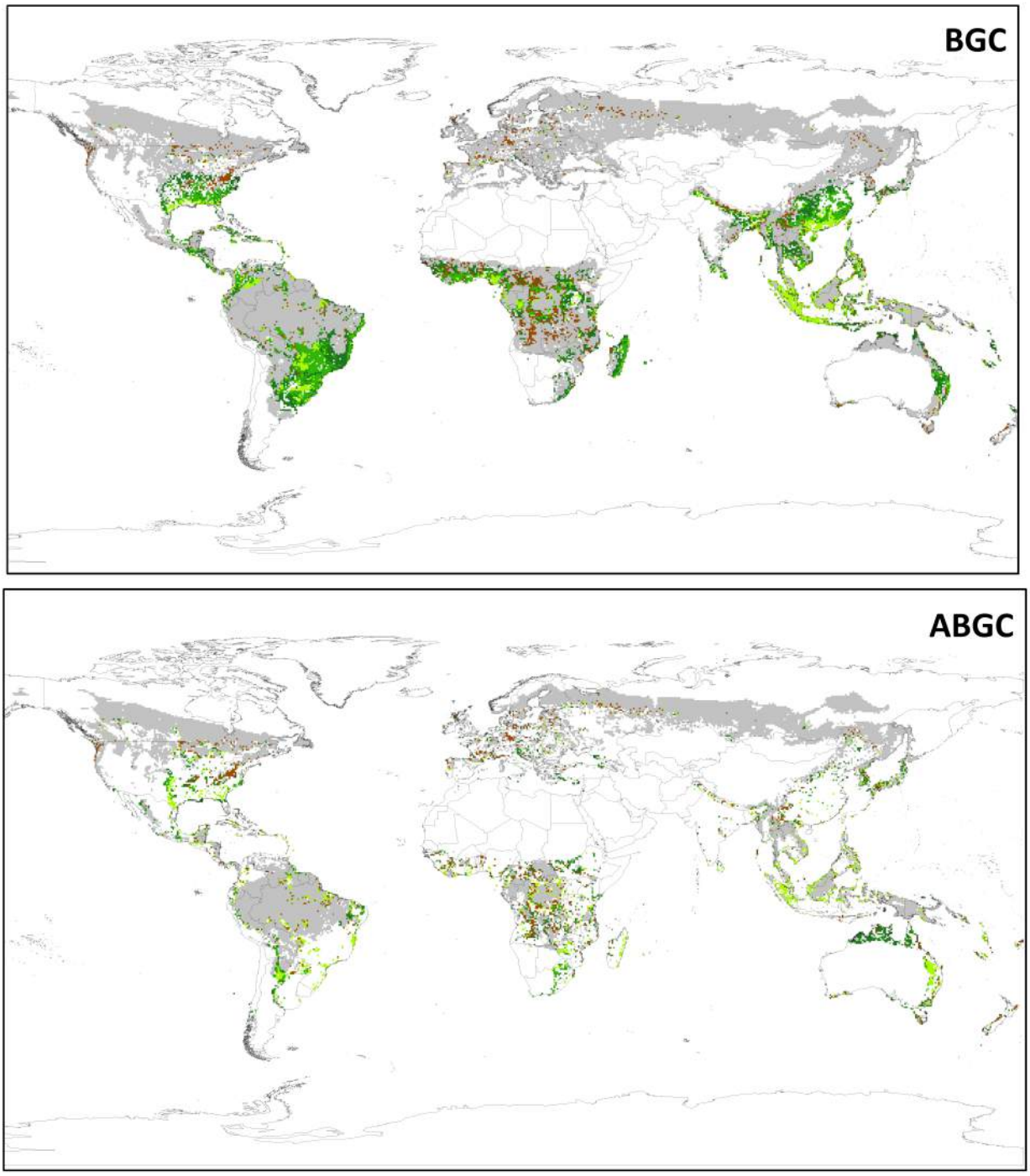

Figure 6: Global spatial distribution of $EF_{land-use}$

In the BGC, the global distribution of the $EF_{land-use}$ is concentrated in areas of high agricultural productivity across all continents. Under the 85 $kgCO_{2eq}/GJ_{primary}$ (35% emission reduction target), the global potential is rather vast across all major global regions with the exception of Europe. At 60% emission reduction target (30 $kgCO_{2eq}/GJ_{primary}$), the low $EF_{land-use}$ are distributed mostly in coastal areas across Asia and North America, specifically in the Yellow River Basin and the Southern Seaboard.

At regional level, low $EF_{land-use}$ of the BGC are correlated with high productivity areas such as agricultural lands (figure 7 and figure 8). In North America, under the 35% ERT a generous part of the south-east of the US is suited for sustainable bioenergy growth. This potential decreases gradually with the increase of the sustainability target, leaving only parts of the Mississippi portal and the Southern Seaboard available for sustainable bioenergy growth under the 60% ERT. The same pattern is displayed also across the Yellow River Basin, which alongside the Gange River delta and the Indonesian archipelago display the highest number of cells under the 60% ERT. In Africa and South America, the sustainable bioenergy production is vastly below the 50% ERT with potential being clustered in the Niger Delta and the Pampean region.

In the ABGC, the low $EF_{land-use}$ become scattered across the continents, and are pushed towards the boundary of major agricultural areas in South America, North America and central Africa (figure 8). Under the 35% emission reduction target (ERT), the highest concentration of grid cells is located in Australia, Asia and the North America, yet when the ERT is raised to 60%, the concentration becomes patchy in areas of Africa, Australia and South East Asia. In Africa and South America, the low $EF_{land-use}$ are vastly dispersed, with only a few notable aggregates in Zimbabwe and south-west Pampas. Asia remains the region with the highest grid cells suited for sustainable bioenergy growth, particularly in Sumatra and the Australian east coast.

In both the BGC and the ABGC, a number of grid cells in the EF maps, display a negative $EF_{land-use}$. The negative EFs are credited to C sequestration, and are concentrated in temperate and tropical forest biomes. The most noticeable ones are located in central Africa, Europe and in the Americas Great Lakes area. This indicates that for these grid cells, it is more beneficial to have bioenergy planted, as compared to resting natural vegetation as the C sequestration rate of the bioenergy is higher than the C sequestration rate of the natural vegetation. There are two non-mutually exclusive dynamics which can lead to C sequestration: negative net C fluxes of the natural vegetation and/or the net C fluxes of bioenergy being higher than the net C fluxes of natural vegetation. Both of these dynamics is supported by literature. First, the climate change impact studies on mature boreal and tropical forest biomes (Parmesan & Yohe, 2003; Betts et al., 2004; Bonan, 2008), reckon that due to climate change induced biome sifts, mature forests are likely to lose C over time, rather than accumulate it. Bonan (2008) argues that "Siberian forests may collapse in some areas and become evergreen [forests] towards the north" (p. 1447), while evergreen forests may "lose some of the evergreen trees and shift towards deciduous [forest]" (ibid.). In the case of tropical forest, biome shifts are likely to "initiate positive climate feedbacks, leading to [net C] loss" (ibid.). Second, degraded lands where perennial crops are cultivated improve soil fertility and reduce soil erosion, dispersion and leaching (Lal, 2001; Lal, 2004; Lal, 2009) thus, are prone to accumulate C and return a positive net C flux as compared to natural vegetation.

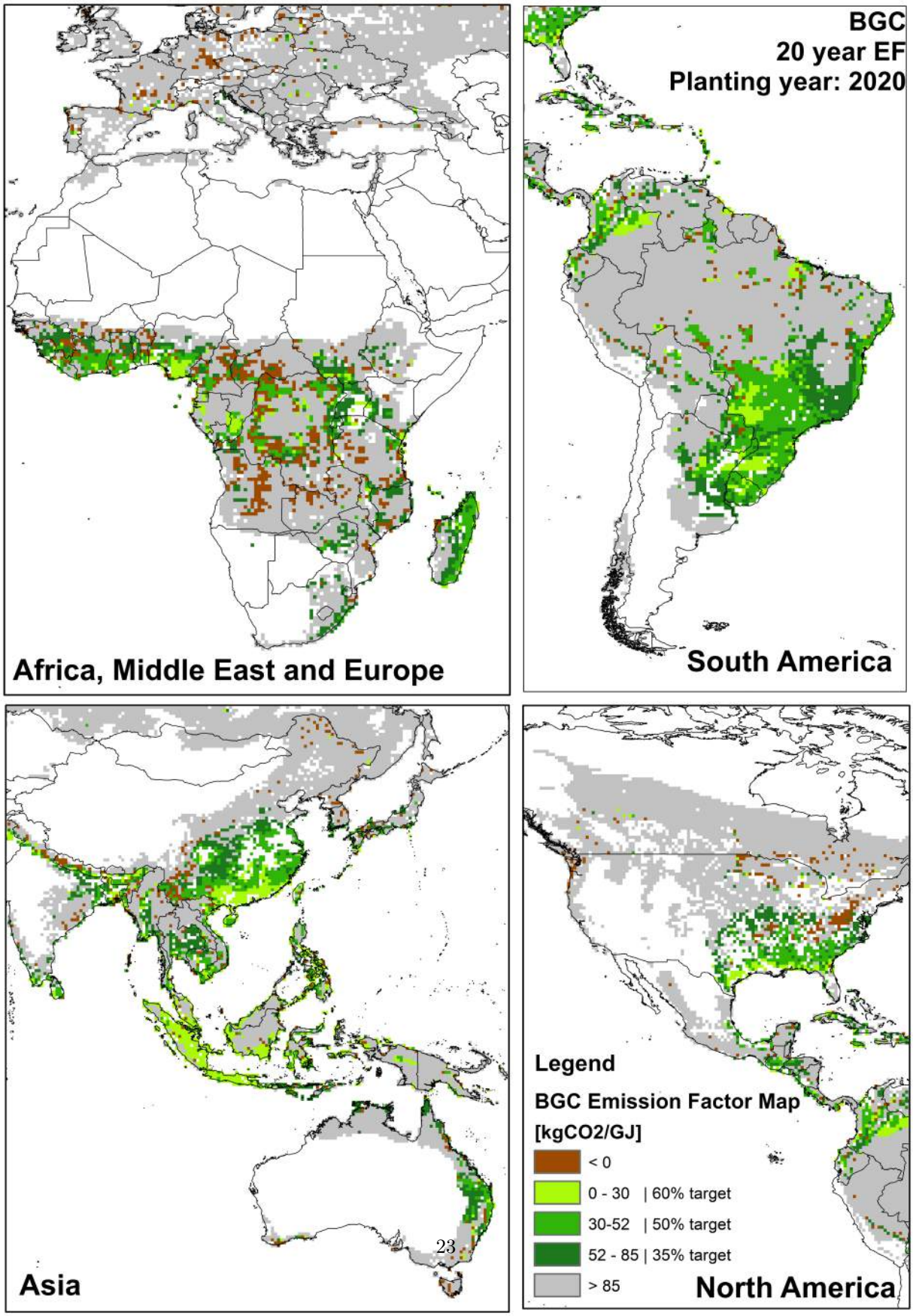

Figure 7: $EF_{land\text{-}use}$ regions map-BGC

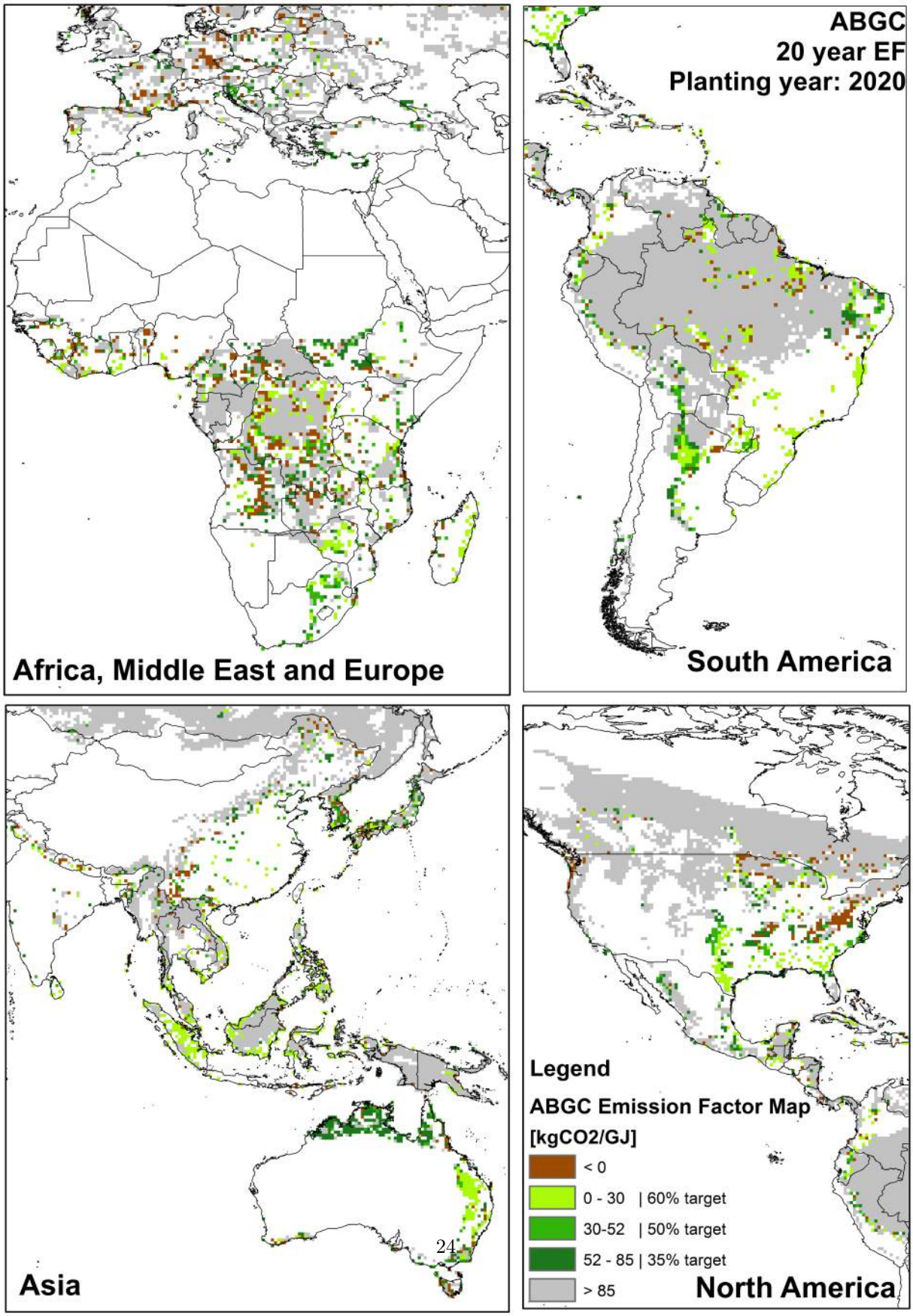

Figure 8: $EF_{land\text{-}use}$ regions map-ABGC

5.1.3 Emission factors supply curves

The land-use based EFSC are an aggregate way of viewing the spatially specific EFs (figure 9 left), at global, regional and biome level. At each spatial level, the EFs are relevant within the EU ERT as displayed in figure 9 - (right), and inventoried in table 8. The bioenergy potentials between the two cases are comparable in terms of their order of magnitude, and correlate with the spatially specific results. The curves (figure 9 - left) indicate that there are significant areas with very high EFs returning low potentials. EFs are a function CO_2 emissions and bioenergy potentials. As bioenergy potentials are computed from biomass yields, which do not vary considerably over time, it can be argued that the high EFs are due to CO_2 emissions. These emissions are more likely type 2 and stem from either baseline C stock changes or LUC significant C stock losses. These areas deliver a marginal increase in mean annual bioenergy potential lower than the $EF_{land-use}$ increase, which means that their added potential is negligible.

Under the 35% ERT threshold (figure 9 - right), the bioenergy potential of the two cases is assessed to be considerable, with potentials decreasing by a factor of 4 (BGC) and 2 (ABGC) towards the 60% ERT threshold (table 8). It is interesting to note that the BGC and the ABGC EFSCs cross each other below the 60% ERT threshold, which is peculiar because there should have always been agricultural lands to mark the difference between the cases.

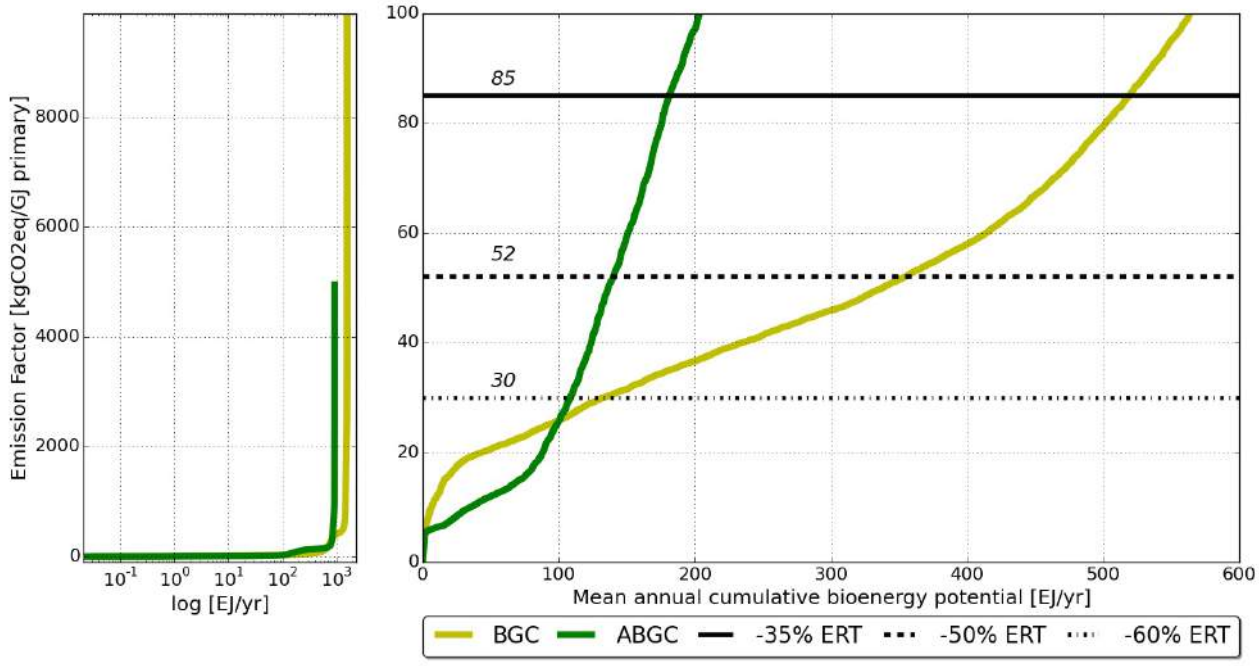

Figure 9: Global EFSC displaying the mean annual cumulative bioenergy potential within given EFs. (left) EFSC display the global potential for the BGC and the ABGC; (right) EFSC under the ERTs for the BGC and the ABGC

Table 8: Inventory of annual mean cummulative bioenergy potential at global level(BGC and ABGC) under EU RED ERTs (35%, 50% and 60%)

	35% ERT	50% ERT	60% ERT
BGC [EJ/yr]	517	354	130
ABGC [EJ/yr]	182	139	108

*ERT= emission reduction target

Broken down into regions, the EFSCs surface the regional variability in potential bioenergy supply. The spatial variability displayed in figure 11 is graphed to emphasize the aggregate potential of the BGC and the ABGC at given $EF_{land-use}$ (table 9). The EFSC of Europe and North America display the steepest slopes amongst regions, indicating that at different $EF_{land-use}$ the potential increase in bioenergy potential is meager. The main causes, for this low bioenergy potential vis-a-vis $EF_{land-use}$, is induced by high CO_2 emissions coming from either the displacement of rich C stock vegetation in the baseline, or considerable C stock loss as a consequence of LUC. Determining the exact source of these CO_2 emissions is a spatially specific exercise. One example are forested areas in the Northern latitudes, which because of their rich C stock, generate a carbon debt unable to be recovered within less than a decade (Wise et al., 2015) if they were displaced for bioenenrgy crop growth. Another example is bioenergy crop growth in areas prone to erosion, such as the European plains.

The EFSCs of South America, Asia and Africa, the regions with the highest number of grid cells under the assigned biofuel sustainability thresholds, display smoother curves. These curves intersect each other at different bioenergy potentials, named here trade points, which indicate the $EF_{land-use}$ level at which a one region substitutes each other in terms of $EF_{land-use}$. This can be interpreted as the bioenergy potential of Asia above the 40 $kgCO_{2eq}/GJ_{primary}$ is less sustainable as compared to that of South America above this EF.

Under the scrutiny of sustainability criteria, bioenergy EFs should not exceed the fossil fuel EF threshold. In the ABGC as compared to the BGC, the lesser land availability for bioenergy production is reflected in the overall potentials which are 40-80% lower between ERTs (Table 9). This returns an overall bioenergy potential of 517EJ/year in the BGC and 182EJ/year in the ABGC, in below the 35% ERT. These potentials are slashed by a factor between 2 to 3, when the ERT is increased to 60%. The overall ranking of the regions in term of their potentials is closely paralleled between the BGC and the ABGC, with South America delivering highest potentials under the 35% ERT and the 50% ERT, when it is taken over by Asia in the BGC, for the 60% ERT. Despite this being the case in the BGC, this ranking does not hold for the ABGC, where South America delivers best potentials overall.

Table 9: Inventory of annual mean cumulative bioenergy potentials at regional level (BGC and ABGC); expressed in [EJ/yr]

	Bioenergy potential under the 35% ERT [EJ/yr]		**Bioenergy potential under the 50% ERT** [EJ/yr]		**Bioenergy potential under the 60% ERT** [EJ/yr]	
	(BGC)	(ABGC)	(BGC)	(ABGC)	(BGC)	(ABGC)
S America	198	53	136	43	36	41
SE Asia	120	62	92	48	54	36
Africa	109	39	59	30	17	21
N America	41	19	26	13	7	8
Europe	2	6	1	2	1	1
Other	47	3	4	3	15	1
TOTAL	**517**	**182**	**354**	**139**	**130**	**107**

*ERT= emission reduction target

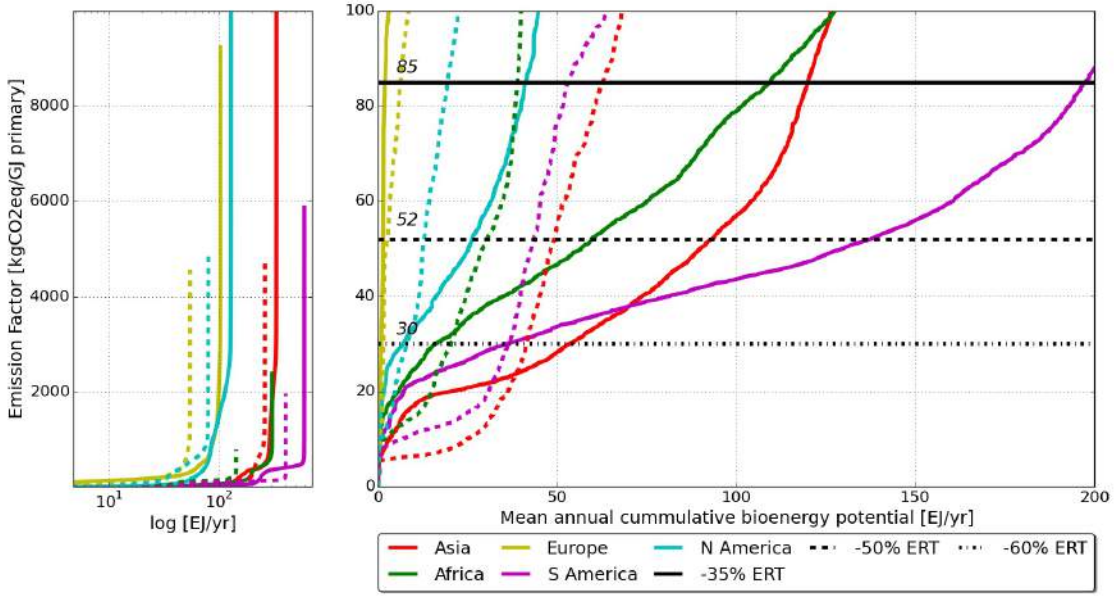

Figure 10: Regional EFSCs; (left) Aggregate EFSCs with full potential display. The full lines indicate the BGC and the dotted lines indicate the ABGC; (right) regional EFSC indicating the emission reduction targets (ERT) thresholds under the biofuel sustainability criteria of EU RED for the BGC and the ABGC.

Broken down into the most representative biomes, the EFSCs can highlight which vegetation type is best suited for land-use conversion, under the assumptions of this assessment. The spatial variability displayed in figure 11 is graphed and inventoried to emphasize the aggregate potential of the BGC and the ABGC at given $EF_{land-use}$ thresholds. The main observation which stems from figure 11, and the associated inventory (table 10), is that in both analyzed cases, grassland remains the dominant biome preferred for land-use conversion for bioenergy growth, at most ERT EF thresholds. The potential from grassland conversion is reduced to half in the BGC when the ERTs are applied, from 146EJ/year (35% ERT) to 68EJ/year (60% ERT). The trade point between the grassland and temperate forests, at EF=76 $kgCO_{2eq}/GJ_{primary}$, which can is attributed to the IPCC soil loss inputs in sub-tropical areas, where grasslands are modeled to incur high rates of C loss due to soil erosion. In the ABGC the grassland mean annual bioenergy potential varies little among the ERTs, between 61EJ/yr (35% ERT) and 53EJ/yr (60% ERT).

Amongst forest biomes, temperate forests return high potentials as compared to tropical and boreal forests. Temperate forests have the lowest C stock accumulations in both the above and below ground pools (Malhi et al., 1999), which is why the C debt repayment is quickest for this forest type. Alongside this, the yield potentials for the areas where temperate forests are located is generous, which is why this biome type provides rather high potentials. Under strict ERTs (60% ERT), temperate forest are modeled to be able to deliver at most 18EJ/year. Tropical areas are, under soil and climatic conditions, best suited for growth of biomass. Despite tropical forests being rich C stocks, the high bioenergy yield potential of the associated areas where they are planted, makes their $EF_{land-use}$ and associated bioenergy potentials better than the ones of boreal forests. Boreal forests, despite having low C stock in the vegetative part, they store the highest amount of C in the below ground C pools, which is why the CO_2 emissions from boreal forest clearance for bioenergy growth would be highest among biomes. Correlated with very low yields in high latitudes, this biome type is the least suited for LUC for bioenergy growth.

Although modeled, shrublands return no bioenergy potential in the results of this analysis. As biome type, shrublands are deemed to be preferred for land-use conversion for bioenergy growth after grasslands, because their C stocks content (Mellilo et al., 2009). The poor bioenergy potential of shrublands in this analysis is sourced in the IMAGE input data. A parallel between the land-use map and yield potential maps indicate that shrublands have very low if any yield potential.

Table 10: Inventory of annual mean cumulative bioenergy potentials at biome level (BGC and ABGC); expressed in [EJ/yr]

	Bioenergy potential under the 35% ERT [EJ/yr]		**Bioenergy potential under the 50% ERT** [EJ/yr]		**Bioenergy potential under the 60% ERT** [EJ/yr]	
	(BGC)	(ABGC)	(BGC)	(ABGC)	(BGC)	(ABGC)
Grassland	146	61	125	56	68	53
Shrubland	0	0	0	0	0	0
Temperate forest	155	47	104	31	34	18
Tropical forest	64	26	16	12	5	4
Boreal forest	1	1	1	1	1	1
Other	151	47	108	39	22	31
TOTAL	**517**	**182**	**354**	**139**	**130**	**107**

*ERT= emission reduction target

The results of the base case offer an overview of the aggregate bioenergy potentials at given EFs, how this is broken down among regions and biomes. These results are generated under the assumption that the land conversion for biomass growth takes place in 2020, with a bioenergy transition period of 20 years. Both the

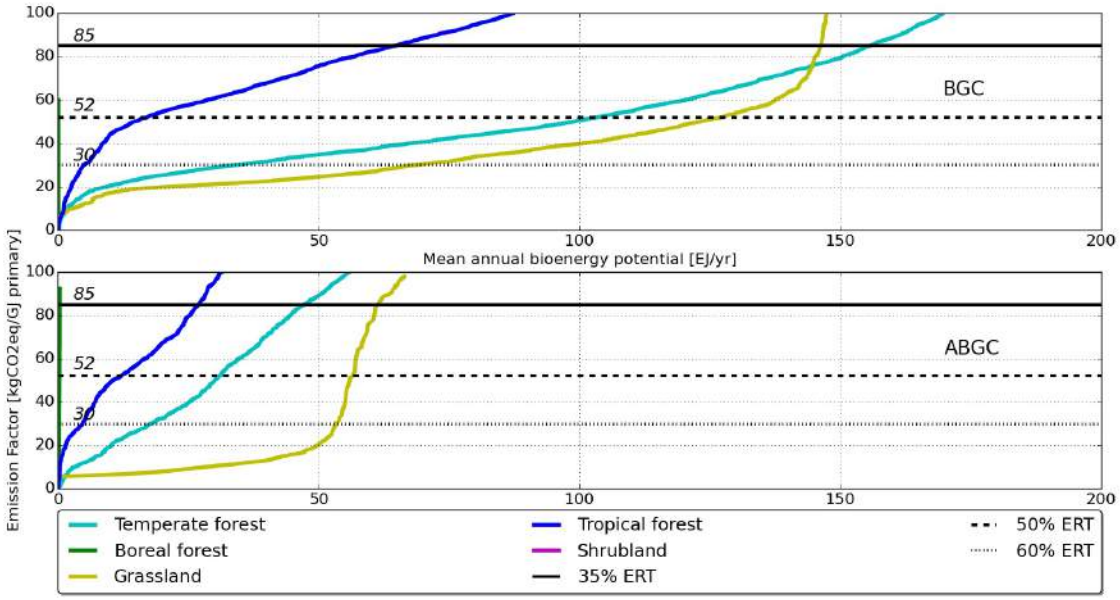

Figure 11: Biome EFSCs; (upper) biome EFSC indicating the emission reduction targets (ERT) thresholds under the biofuel sustainability criteria of EU RED for the BGC; (lower) biome EFSC indicating the emission reduction targets (ERT) thresholds under the biofuel sustainability criteria of EU RED for the ABGC.

transition period and the planting year can alter the spatial distribution of $EF_{land-use}$ and shift the EFSCs.

5.2 Transition period variation

The $EF_{land-use}$ of bioenergy is strongly influenced by the number of years the bioenergy crops are cultivated on the same plot of land. The base case shows results for a 20 year transition period (20EF), yet a 10 or 30 year transition period (10/30 EF) show shifts in the EFSCs. In both the BGC and the ABGC, the 30 EF delivers a higher potential as compared to the 20 EF, while the 10 EF delivers a lower potentials (figure 12 upper left, lower left). For both the shorter and the lower transition periods, type 1 emissions have the strongest effect on the EFSC. For the shorter transition periods, the cumulative production of biomass is lower and thus generates higher $EF_{land-use}$. Adversely, for the long transition periods the dynamics works opposite. Analyzed under the EU RED ERTs, the BGC 30 EF delivers a bioenergy potential of about 600EJ/yr under the 35% ERT, but shrinks by a factor of 3 when the ERT is increased to 60% (figure 12 - upper right). For the ABGC, the bioenergy potential reaches nearly 300EJ/yr under the 35% ERT, and lowers down to about half under the 60% ERT (figure 12 lower right).

It is worth noting that in the BGC the spread between the 10 EF and the 20EF curves is about 20% lower than the base case (at the 35% ERT); while the spread between EF20 and the 30EF curve is about 5% higher (at the 35% ERT), than the base case which mean that the 10EF has a stronger impact than the 30EF.

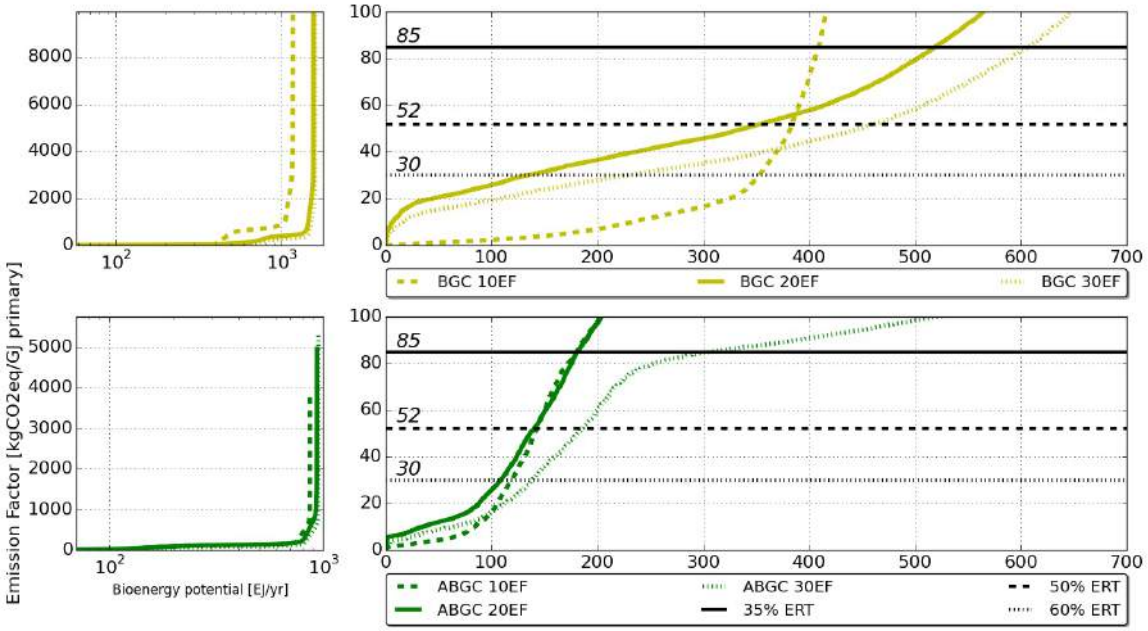

Figure 12: EFSC for the 10-20-30 EF. (upper left) Aggregate EFSC with full potential display for the BGC, displayed in log scale; (upper right) EFSC under the ERTs for BGC; (lower left) Aggregate EFSC with full potential display for the ABGC, displayed in log scale; (lower right) EFSC under the ERTs for ABGC

5.3 Planting year variation

In both assessed cases, postponing the plantation of bioenergy delivers higher $EF_{land-use}$, thus planning in 2010 is better than planting in 2030. The reason for these results is attributed to baseline input data, specifically C stocks. As global C stocks decrease over time as a consequence of biome shifts, they impact positively the EFs. The decrease in C stocks of natural vegetation over time determines the type 2 emissions to increase, which in turn raise the $EF_{land-use}$. Over time, this effect propagates to a large number of cells, most of which are located in sensitive climate hotspots such as ecotones, and specifically ecoclines. A number of influential ecological sensitivity studies (Bergengren et al., 2011; Hirota et al., 2011) reckon that vegetation cover is projected to undergo shifts in areas such as equatorial Africa, Madagascar, Himalayan and Tibetan Plateau, North Americas Great Lakes and in the Northern Hemisphere high latitude, particularly boreal forests (taiga) ecotones, which correlate well with the results of this study.

Opposite to the biome shift argument, yields improvements in the future can counteract the increase of the $EF_{land-use}$. As yields improve they lead to higher bioenenrgy potential which can lead to a decrease in the EFs. Because yields improve, on average, by 1%/yr, this leads to a 1% improvement in bioenenrgy potential on a yearly basis. Global C stocks decrease at a faster rate that the yield increase, thus counteracting the yield improvements effect on EFs.

Analyzed under the EU RED ERTs, for the BGC, planting in 2010 delivers bioenergy potential of about 615EJ/yr under the 35% ERT, but shrinks by a factor of 5 when the ERT is increased to 60% (figure 13 - upper right). For the ABGC, the bioenergy potential reaches nearly 217EJ/yr under the 35% ERT, and lowers down to about half under the 60% ERT (figure 13 lower right).

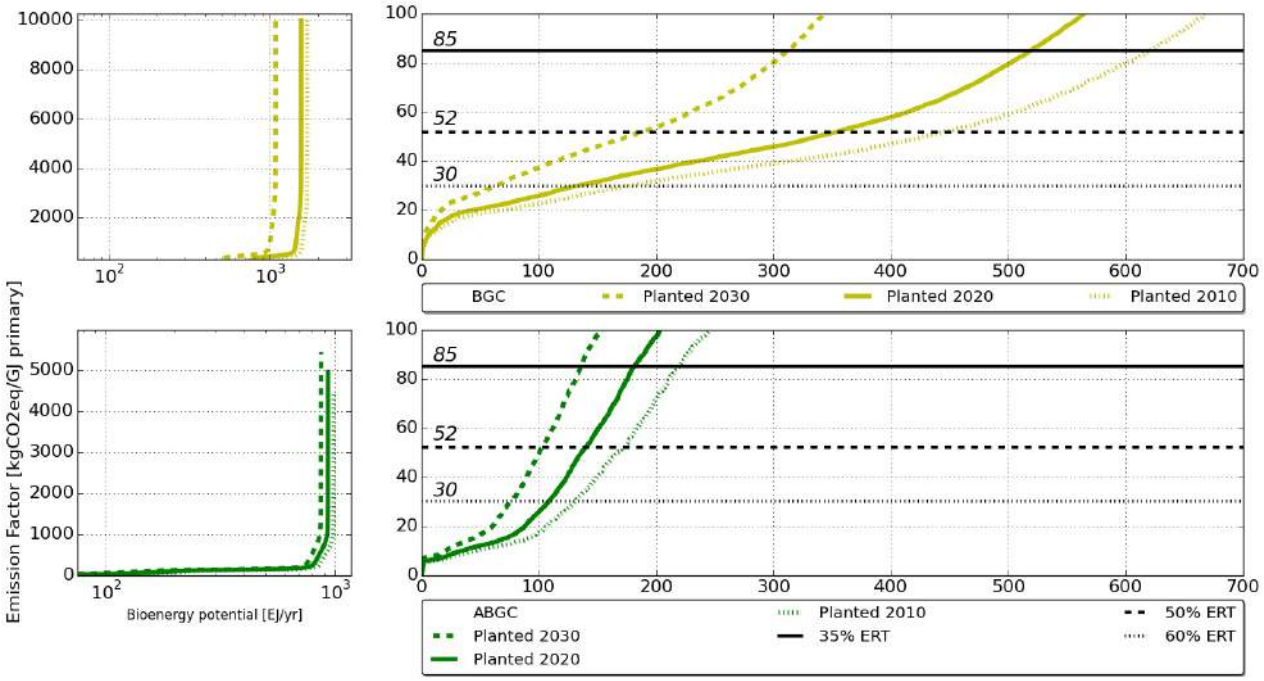

Figure 13: EFSC for the planting year variation 2010-2020-2030. (upper left) Aggregate EFSC with full potential display for the BGC, displayed in log scale; (upper right) EFSC under the ERTs for BGC; (lower left) Aggregate EFSC with full potential display for the ABGC, displayed in log scale; (lower right) EFSC under the ERTs for ABGC

The variation in planting year surfaces an increased number of grid cells sequestering C in the North Americas Great Lakes, Europe and particularly in the Congo River basin. This indicates that in these areas it is ever more beneficial to have bioenergy planted because the C sequestration rate of the bioenergy is higher than the C sequestration rate in the natural vegetation. This can be the case for degraded lands where perennial crop cultivation improves soil fertility and reduce other soil degradation processes such as soil erosion, dispersion and leaching (Lal, 2001; Lal, 2004; Lal, 2009).

6 Discussion

Under climate with no mitigation measures taken throughout the projection period, IMAGE display a strong northwards biome shift, which generates across time, a decrease in the above and soil carbon pools of the natural vegetation case. Such an outcome is in line with more recent ecological sensitivity studies which argue that forest and other rich C stocks are projected to decrease in biome boundary areas due to climate change inertial effects (Bergengren et al., 2011; Hirota et al., 2011). Alongside this aspect of the input data, IMAGE generates the yield potentials for the second generation bioenergy crops as a suitability average of the pre-allocated crops indexed globally with on average 1% per year (Stehfest et al., 2014). This later on factored into the computation of the bioenergy potential. The yield increase relies on regional differentiation such that areas like USA, which already benefit from high yields, would not result in future inflated potentials. These two aspects, the integration of climate change effects and the regional differentiation of yield improvements distinguish IMAGE from other IAMs, for the better.

In the carbon accounting for the bioenergy cases, this assessment makes use of IMAGE derived land-use data and IPCC below-to-above ground ratio to generate the C stocks of the grassy crops. These two datasets are both rather coarse, with IMAGE accounting for 20 land-use types and the below-to-above ground ratio provided in the IPCC guidelines accounting for only 5 vegetation types. As the below-to-above ground ratio can be susceptible to agro-ecological conditions it is safe to mention that the computed C stock value could be over or underestimated. Assessments of the below-to-above ground ratio for grassy crops are acknowledged to vary not just among grass types, but also for the same grass type at different climate zones (Kwabiah et al., 2002; Dohleman et al., 2012; Kuyah et al., 2012). Alongside the below-to-above ground ratio this assessment uses IPCC guidelines specifically in the carbon accounting step in the form of input factors as an additional factor in C stock computation for the bioenergy cases. In the IPCC guidelines these factors rely on a rather rudimentary description which can render questionable the choices of land management factors (land use, input and land management). Moreover, these factors are not region specific to account for the variability of climatic, soil, and other region specific parameters. As biomass C stock changes are a major contributor to the GHG balance of bioenergy is it relevant to emphasize that any degree of specificity improves the EF estimates.

As the 20 land-use types provided by IMAGE are deemed coarse, it is fair to mention, that this is still state-of-the-art data amongst IAMs. In comparison, a recent study on the assessment of C payback times for different bioenergy crops was constructed on 2 land-use types (Elshout et al., 2015). More detailed land-use classes would improve the results, and contribute to the refinement of the study.

Land-use cover is a major component of the C stock estimates in this assessment. With respect to the IMAGE land-use specific inputs, it is relevant to mention that this study does not filter out urban areas, protected areas, and other land cover types which through their destination are not relevant to be accounted in the bioenergy crop growth potential. To increase the accuracy of this assessment these land-use types need to be discarded from the land-use. Alongside this, increasing the number of land use classes in the input maps and increasing the spatial resolution of the maps can deliver finer results to the assessment by making it sensitive to land-use plots smaller than the 0.5x0.5 degree cell. It is to be acknowledged that finer resolution needs to be supplemented by data quality, to add value to the overall results.

Besides the spatial resolution, the 10 year time steps temporal resolution is subject to scrutiny as it is limited in accounting for yearly dynamics in land use shifts. Currently, the assessment assumes 10 year time steps in the analysis, but yearly time steps can more accurately represent land-use conversions, and thus better account for the C stock changes and EF estimates. An example of a sensitive transition is the conversion from natural vegetation, in the baseline case, to the second generation bioenergy crops, in the planting year. This transition can assume biomass being planted in 2020. The first year, 2021, can be classified as cropland because of the necessary land management activities such as plowing and tillage which prepare land for cropping. It is from 2022, the first year post the transition that the land-use can be classified as bioenergy

crops, and stay in this class for the next 19 years. Additionally, yearly resolution can make it easier to map also LUC during the transition period, as currently the assessment assumes that grid cells stay in the same land-use category for 10 years, between the time steps. Solving for the 10 year time steps limitation would yield twofold improvements in the assessment, first mapping land-use conversion for bioenergy analysis, and second, by improving the spatial resolution of land use dynamics.

This assessment provides the framework for deriving land-use driven CO_2 emissions of bioenergy, but CO_2 is not the only GHG emission associated with the bioenergy production. On the one hand, agricultural inputs release emissions such as nitrous oxide (N_2O) and methane (CH_4) stemming from nitrification and de-nitrification processes in the soil. These emissions are a consequence of "mineral fertilization, organic amendment and organic residues" (van der Hilst et al., 2014). These processes added to the GHG emission inventory increase the EF balance of bioenergy. On the other hand, only by adding the chain GHG emission associated with the primary biomass conversion can make the life cycle bioenergy EF complete. The comparison with life-cycle inventory fossil fuel EFs puts into perspective the results at aggregate levels.

The results of this assessment generate a number of discussion points. The CO_2 emission profile constructed in this assessment is similar to that of other studies (IPCC, 2006; Wise et al., 2015). This profile signals that the main source of emissions is linked to transition from one land cover to another. The emission calculation relies on C stock changes in the baseline input data, which have the strongest effect on the EFs. An example of this occurrence is surfaced in the EFSC of biomes of the base case analysis. Here, the temperate forests ranked second in terms of EFs, after grassland as their C stocks are lowest among forests, while the agro-ecological and climatic conditions offer a good suitability for yield potentials. In this example, both the C stock input data and the yield potentials influence the outcome of the resulting $EF_{land-use}$.

With respect to the assessment, a number of positive aspects need to be highlighted. First is the spatial specificity of the analysis, relying on raster inputs and performing the processing in a geo-spatial environment. Second, unlike the vast majority of the bioenergy scientific literature which looks at first generation bioenergy crops, this assessment looks at the bioenergy production potential from second-generation biomass, which has proven to offer energetic, environmental and economic advantages over first-generation sources (Hill et al., 2006; Melillo et al., 2009; Schmer et al, 2009; Dunn et al., 2013). A third added value of this assessment methodology is that the analysis is performed at global level, thus offering global spatially specific $EF_{land-use}$.

7 Conclusions

The sustainability of bioenergy has been severely scrutinized in academia, policy and the corporate arena for the past half a decade. The main criticism brought to bioenerg hinges on the LUC emissions. Because of their strong spatial specificity and the wide range of socio-economic interactions, require extensive mapping efforts and have high data input requirements. Direct and indirect LUC effects of the bioenergy system are genuinely cross boundary dynamics, which can only be fully mapped at global level. Alongside this, high computation power, global coverage data and access to available and reliable C stock data act as limiting factors in an effort to fully map the LUC GHG emissions at a global level. This study addressed this gap by developing and applying a methodological framework to spatially specific derive the LUC induced EFs of bioenergy.

The main finding of this assessment is that bioenergy land-use EFland use are highly spatially dependent, with baseline C stocks, soil C loss and bioenergy potentials, accounting as main contributor in its variability. Between the bioenergy potential and the EF there is an inverse relation, as for example the effect of yield improvements which drive down EFs. The magnitude of C stocks fluxes depends on the type of vegetation displaced as well as the C stock, loss or accumulation, over time. Although generally low, soil C loss can increase the EF in areas with high erodible soils.

The biophysical processes involved in the C stock changes relate to climatic effects and soil carbon loss, the latter being mostly caused by erosion. Climate effects trigger biome shifts in ecotones where natural vegetation C uptake rates are projected to decrease. The C stock uptake rate influence the C fluxes, leading to increased CO_2 emissions when natural vegetation is cleared for bioenergy crop growth. The soil C loss is triggered by land-cover removal, and it is increased through agricultural management practices such as tillage. This is can be enhanced by soil characteristics and topography. Some of these risks are mitigated through the plantation of lingnocellulosic perennial crops which improve soil C accumulation.

The global EFland use maps provide a comprehensive view of the bioenergy potential and associated CO_2 emissions. In the BGC, the vastly available potential spreads over vast areas in the Cerrado region (South America), the Mississippi portal and Southern Seaboard (North America), the Congo River Basin and Madagascar (Africa) and the Yellow River Basin (Asia). For this analyzed case, the sustainable potential under the current ERTs (-35% emission reductions) can reach as high as 517EJ/yr, with the highest potential being recorded in South America (198EJ/yr) and Asia (120EJ/yr). Putting these figures into perspective, the IEA indicates that the total global primary energy supply in 2014 was 550EJ/yr (IEA, 2014). Part of this supply can be sustainably supplied in a sustainable manner from lignocellulosic bioenergy. Under the same sustainability criteria, these potentials are tempered down in the ABGC, which displays a maximum global bioenergy potential of 182EJ/yr. The regional potentials are also reduced, to 62 EJ /yr in Asia and 53EJ/yr in Asia. The reduction of the global cumulative potential means also a shrinkage in the number of grid cells available for bioenenrgy production, which becomes concentrated in Southern Seaboard (North America), La Pampa (South America), Eastern African coast and the coastal area of the Yellow River Basin (Asia).

Through both analyzed cases, grassland remains the dominant biome preferred for land-use conversion for bioenergy growth, at most ERT EF thresholds. The potential from grassland conversion is reduced to half in the BGC when the ERTs are applied, from 146EJ/year (35% ERT) to 68EJ/year (60% ERT). Amongst forest biomes, temperate forests return high potentials as compared to tropical and boreal forests. This potential is due to the low C stocks of temperate forests as compared to other forest types, and the land suitability reflected in the yield potential of the areas where temperate forest is stationary.

The two alterations tested in the base case worked with transition period variation and planting year variation. The choice of bioenegy transition period has an impact on the $EF_{land-use}$, as the EFs are driven by the type 1 emissions. For a shorter transition period, the cumulative production of biomass is lower than that

of the base case, and thus generates higher $EF_{land-use}$. Adversely, for the long transition periods the effect on the $EF_{land-use}$ is opposite. The plantation year variation results indicate that postponing the plantation of bioenergy delivers higher $EF_{land-use}$, hence planting now delivers better potentials. The explanation for these results is attributed to baseline input data, specifically C stocks. As global C stocks decrease over time as a consequence of biome shifts, they impact positively the EFs. The decrease in C stocks of natural vegetation over time determines the type 2 emissions to increase, which in turn raise the $EF_{land-use}$.

There are a number of aspects on which further research can be conducted:

- Filters for other parameters such as biodiversity, water stress and risk of erosion. Despite high potential being widely distributed across a number of regions in North America, South America, Africa and South-East Asia, these regions could be under biodiversity or water stress. Such areas could be re-evaluated under filters for biodiversity, water stress and protected areas.
- Climate change scenarios. This assessment is build-on a climate change scenario which assumed no mitigation measures will be taken to address climate change. In the same line or reasoning, further research could be carried out for different climate change scenarios/levels, in order to better understands the on what conditions EFs deliver higher or lower values, and what does it mean for bioenergy policy.
- EF reduction methods. Bioenergy $EF_{land-use}$ can potentially be reduced through either lower emissions and/or improved bioenergy potential. For emissions management, soil carbon retention and accumulation methods can be investigated to assess how they perform relative to the EF. For bioenenrgy potential improvement methods, agricultural practices aimed at yield improvements could be conducted to assess their effect on the EF. The yield increase methods include planting of high yielding varieties and complete harvesting, while soil carbon retention and accumulation practices include addition of nutrients, salinity reduction practices and no tillage for soil erosion avoidance.
- Complete the land use change GHG emissions inventory. Besides CO_2 emissions associated with biomass clearing, environmental assessment studies also could account for other GHG emission such as N_2O. Closely linked to primary biomass productivity are nitrogen emissions, which stem from primary biomass intensification and use of fertilizers. N_2O forms during soil processes such as nitrification and denitrification, from where they are emitted into the atmosphere (van der Hilst et al., 2013). It is relevant to point out that N_2O emissions are amendable to "local conditions such as agricultural land use, soil type and N-origin" (p. 397), and thus require spatial specific mapping.

8 References

Aalde, H., Gonzalez, P., Gytarsky, M., Krug, T., Kurz, W., Lasco, R., ... Verchot, L. (2006). Chapter 2 - Generic Methodologies Applicable to Multiple Land Use Categories. In 2006 IPCC guidelines for national greenhouse gas inventories. Geneva: Intergovernmental Panel on Climate Change.

Ahlgren S, Di Lucia L (2014) Indirect land use changes of biofuel production a review of modelling efforts and policy developments in the European Union. Biotechnology for Biofuels, 7-35.

Bain RL. (2007) World biofuels assessment, worldwide biomass potential: technology characterizations. Golden, CO, USA: National Renewable Energy Laboratory; (NREL/MP-510-42467).

Barona E, Ramankutty N, Hyman G, Coomes OT (2010) The role of pasture and soybean in deforestation of the Brazilian Amazon. Environ. Res. Lett. 5 024002.

Bergengren, J., Waliser, D., & Yung, Y. (2011). Ecological sensitivity: A biospheric view of climate change. Climatic Change, 107(3-4), 433-457.

Beringer, T., Lucht, W., & Schaphoff, S. (2011). Bioenergy production potential of global biomass plantations under environmental and agricultural constraints. GCB Bioenergy, 3(4), 299-312.

Berndes, G., Hoogwijk, M., & Broek, R. (2003). The contribution of biomass in the future global energy supply: A review of 17 studies. Biomass and Bioenergy, 25(1), 1-28.

Betts, R., Cox, P., Collins, M., Harris, P., Huntingford, C., & Jones, C. (2004). The role of ecosystem-atmosphere interactions in simulated Amazonian precipitation decrease and forest dieback under global climate warming. Theoretical and Applied Climatology, 78, 157-175.

Bonan, G. (2008). Forests and Climate Change: Forcing, Feedbacks, and the Climate Benefits of Forests. Science, 320, 1444-1449.

Bondeau, A., Smith, P., Zaehle, S., Schaphoff, S., Lucht, W., Cramer, W., Gerten, D., Lotze-Campen, H., Muller, C., Reichstein, M., Smith, B. (2007). Modelling the role of agriculture for the 20th century global terrestrial carbon balance. Global Change Biology 13(3), pp. 679-706.

Calvin, K., M. Wise, D. Klein et al. (2013), A multi-model analysis of the regional and sectoral roles of bioenergy in near-term and long-term carbon mitigation. Climate Change Economics

Cherubini, F., and Strmman, A.H. (2011) Life cycle assessment of bioenergy systems: State of the art and future challenges. Bioresource Technology 102(2), 437-451.

Clarke, L., Edmonds, J.A., Pitcher, H.M., Reilly, J.M., Richels, R.G. (2007) Scenarios of Greenhouse Gas Emissions and Atmospheric Concentrations. Sub-report 2.1 A of Synthesis and Assessment Product 2.1 by the U.S. Climate Change Science Program and the Subcommittee on Global Change Research. Department of Energy, Office of Biological and Environmental Research, Washington DC, USA

Daioglou, V., B. Wicke, A. Faaij et al. (2014), Competing uses of biomass for energy and chemicals: Implications for long-term global CO2 mitigation potential. GCB - Bioenergy, pp.14.

DeCicco JM (2013) Biofuels carbon balance: doubts, certainties and implications. Climatic Change 121, 801814.

Dohleman, F., Heaton, E., Arundale, R., & Long, S. (2012). Seasonal dynamics of above- and below-ground biomass and nitrogen partitioning in Miscanthus giganteus and Panicum virgatum across three growing seasons. Glob. Change Biol. Bioenergy GCB Bioenergy, (111), 534-544.

Dornburg, V., Vuuren, D., Ven, G., Langeveld, H., Meeusen, M., Banse, M., ... Faaij, A. (2010). Bioenergy revisited: Key factors in global potentials of bioenergy.Energy & Environmental Science, 3, 258-258.

Dunn, J., Mueller, S., Kwon, H., & Wang, M. (2013). Land-use change and greenhouse gas emissions from corn and cellulosic ethanol. Biotechnology for Biofuels, 6, 51-51.

ECN Phyllis Database, 2014 (accessed 10 March, 2015)

Edwards, R., Larive, J., Rickeard, D., & Weindorf, W. (2014). Well-to-wheels report version 4.a JEC well-to-wheels analysis : Well-to-wheels analysis of future automotive fuels and powertrains in the European context. (JRC85326 ed.). Luxembourg: Publications Office.

Elshout, P., Zelm, R., Balkovic, J., Obersteiner, M., Schmid, E., Skalsky, R., . . . Huijbregts, M. (2015). Greenhouse-gas payback times for crop-based biofuels. Nature Climate Change Nature Climate Change, 5, 604-610.

EPA. Renewable Fuel Standard Program (RFS2) regulatory impact analysis. (2010) Washington, DC, USA: Environmental Protection Agency; (EPA-420-R- 10-006) European Commission, 2009. Directive 209/28/EC of the European Parliament and of the Council of 23 April 2009 on the promotion of the use of energy from renewable sources and amending and subsequently repealing Directives 2001/77/EC and 2003/30/EC. Retrieved 18/05/2015, from http://eur-lex.europa.eu/legal-content/EN/ALL/?uri=CELEX%3A32009L0028

Fargione, J., Hill, J., Tilman, D., Polasky, S., & Hawthorne, P. (2008). Land Clearing And The Biofuel Carbon Debt. Science,319, 1235-1238.

Fritsche, U., Hennenberg, K., Hnecke, K.(2010) The iLUC Factoras a means to hedge risks of GHG emissions from indirect land use change. ko-Institut working paper. Available at: http://www.oeko.de/oekodoc/1030/2010-082-en.pdf

Gerbens-Leenes, W., Hoekstra, A., & Meer, T. (2009). The water footprint of bioenergy. Proceedings of the National Academy of Sciences, 106(25), 10219-10223.

Groom, M., Gray, E., & Townsend, P. (2008). Biofuels and Biodiversity: Principles for Creating Better Policies for Biofuel Production. Conservation Biology,22(3), 602-609.

Hill, J. (2006). From The Cover: Environmental, Economic, And Energetic Costs And Benefits Of Biodiesel And Ethanol Biofuels. Proceedings of the National Academy of Sciences, 103 (30), 11206-11210.

Hirota, M., Holmgren, M., Nes, E., & Scheffer, M. (2011). Global Resilience of Tropical Forest and Savanna to Critical Transitions. Science, 334(6053), 232-235.

Hoefnagels, R., Smeets, E., & Faaij, A. (2010). Greenhouse gas footprints of different biofuel production systems.Renewable and Sustainable Energy Reviews,14(7), 1661-1694.

Hoogwijk, M., Faaij, A., Eickhout, B., Devries, B., & Turkenburg, W. (2005). Potential of biomass energy

out to 2100, for four IPCC SRES land-use scenarios.Biomass and Bioenergy, 29(4), 225-257.

International Energy Agency (IEA). (2014). CO2 Emissions from Fuel Combustion 2014 (2014 ed., Vol. 1, p. 136). Paris: IEA Statistics.

IPCC (2006) IPCC Guidelines for National Greenhouse Gas Inventories. Prepared by the National Greenhouse Gas Inventories Programme. Eggleston HS, Buendia L, Miwa K, Ngara T and Tanabe K (eds) Published: IGES, Japan. Available at: http://www.ipcc-nggip.iges.or.jp/public/2006gl/

Kim, H., Kim, S., & Dale, B. (2009). Biofuels, Land Use Change, and Greenhouse Gas Emissions: Some Unexplored Variables. Environmental Science & Technology, 961-967.

Klein D., Luderer G., Kreigler E., Strefler J., Bauer N., Popp A., Dietrich J.P., Humpender F., Lotze-Campen H., Edenhofer O. (2013) The value of bioenergy in long-term low- stabilization scenarios: an assessment with ReMIND-MAgPIE. Climatic Change, 123, 705-718.

Kuyah, S., Dietz, J., Muthuri, C., Jamnadass, R., Mwangi, P., Coe, R., & Neufeldt, H. (2012). Allometric equations for estimating biomass in agricultural landscapes: II. Belowground biomass. Agriculture, Ecosystems & Environment, 158, 225-234.

Kwabiah, A., Spaner, D., & Todd, A. (2002). Shoot-to-root ratios and root biomass of cool-season feed crops in a boreal Podzolic soil in Newfoundland. Can. J. Soil. Sci. Canadian Journal of Soil Science, (321), 369-376.

Lal, R. (2001). Potential of Desertification Control to Sequester Carbon and Mitigate the Greenhouse Effect. Storing Carbon in Agricultural Soils: A Multi-Purpose Environmental Strategy, 51(1), 35-72.

Lal, R. (2004). Carbon Sequestration in Urban Ecosystems. Environmental Management, 33(4), 528-544. Lal, R. (2009). Carbon Sequestration in Agricultural Soils. Journal of Soil Salinity and Water Quality, 1(1-2), 30-40.

Lamers, P., & Junginger, M. (2013). The debt is in the detail: A synthesis of recent temporal forest carbon analyses on woody biomass for energy. Biofuels, Bioproducts and Biorefining, 7, 373-385.

Lapola, DM, Schaldach, R, Alcamo, J, Bondeau, A, Koch, J, Koelking, C, Priess, JA (2010). Indirect land-use changes can overcome carbon savings from biofuels in Brazil. Proceedings of the National Academy of Sciences 107, 3388-3393.

Malhi, Y., Baldocchi, D., & Jarvis, P. (1999). The carbon balance of tropical, temperate and boreal forests. Plant, Cell and Environment Plant Cell Environ, 22, 715-740.

Melillo, J., Reilly, J., Kicklighter, D., Gurgel, A., Cronin, T., Paltsev, S., . . . Schlosser, C. (2009). Indirect Emissions from Biofuels: How Important? Science, 326, 1397-1399.

Milazzo, M., Spina, F., Cavallaro, S., & Bart, J. (2013). Sustainable soy biodiesel.Renewable and Sustainable Energy Reviews, 27, 806-852.

Nassar, A., Harfuch, L., Bachion, L., & Moreira, M. (2011). Biofuels and land-use changes: Searching for the top model.Interface Focus, 224-232.

Ostwald M & Henders S (2014) Making two parallel land-use sector debates meet: Carbon leakage and indirect land-use change. Land Use Policy 36, 533-542.

Parmesan, C., and Yohe, G. (2003). A Globally Coherent Fingerprint Of Climate Change Impacts Across Natural Systems. Nature, 412, 37-42.

Popp, A., Lotze-Campen, H., Leimbach, M., Knopf, B., Beringer, T., Bauer, N., & Bodirsky, B. (2011). On sustainability of bioenergy production: Integrating co-emissions from agricultural intensification.Biomass and Bioenergy, 35(12), 4770-4780.

Popp, A., Rose, S., Calvin, K., Van Vuuren, D., Dietrich, J., Kriegler, E. (2014). Land-use transition for bioenergy and climate stabilization: Model comparison of drivers, impacts and interactions with other land-use based mitigation options. Climate Change,123, 495-509.

Rose, S., E. Kriegler, E. Bibas et al. (2014), Bioenergy in energy transformation and climate management. Climatic Change 123, pp.477-493.

Sala, O.E., D. Sax & H. Leslie. (2009). Biodiversity consequences of increased biofuel production. In Biofuels: Environmental Consequences and Interactions with Changing Land Use. R.Howarth & S.Bringezu, (eds), 127137. Cornell University. Ithaca , NY . Available at: http://cip.cornell.edu/biofuels/.

Schmer, M., Vogel, K., Mitchell, R., & Perrin, R. (2008). Net Energy Of Cellulosic Ethanol From Switchgrass. Proceedings of the National Academy of Sciences, 464-469. Searchinger, T., Heimlich, R., Houghton, R., Dong, F., Elobeid, A., Fabiosa, J., ... Tun-Hsiang Yu, T. (2008). Use of US croplands for biofuels increases greenhouse gases through emissions from land-use change. Science, 319(1), 1238-1240.

Sitch, S., Smith, B., Prentice, I., Arneth, A., Bondeau, A., Cramer, W., ... Venevsky, S. (2003). Evaluation of ecosystem dynamics, plant geography and terrestrial carbon cycling in the LPJ dynamic global vegetation model. Global Change Biology, 9(2), 161-185.

Smeets EMW, Faaij APC, Lewandowski IM, Turkenburg WC (2007) A bottom-up assessment and review of global bio-energy potentials to 2050. Progress in Energy and Combustion Science 3, 56-106.

Stehfest, E., Van Vuuren, D., Kram, T., & Bouwman, L. (2014). Integrated assessment of global environmental change with IMAGE 3.0: Model description and policy applications. The Hague: PBL Netherlands Environmental Assessment Agency

van Dam, J., Faaij, A., Hilbert, J., Petruzzi, H., & Turkenburg, W. (2009). Large-scale bioenergy production from soybeans and switchgrass in Argentina. Renewable and Sustainable Energy Reviews, 13, 1710-1733.

van der Hilst F, Verstegen JA, Zheliezna T, Drozdova O, Faaij APC (2014) Integrated spatiotemporal modelling of bioenergy production potentials, agricultural land use, and related GHG balances; demonstrated for Ukraine. Biofeuls, Bioprod. Bioref. In press.

Verburg, R., Stehfest, E., Woltjer, G., & Eickhout, B. (2009). The effect of agricultural trade liberalisation on land-use related greenhouse gas emissions. Global Environmental Change, 19(4), 434-446.

Verchot, L., Krug, T., Lasco, R., Ogle, S., Raison, J., Yue, L. (2006). Chapter 6 - Grassland. In IPCC Guidelines for National Greenhouse Gas Inventories Volume 4 - Agriculture, Forestry and other land-use (1st ed., Vol. 4, pp. 273-320). Geneva: International Panel on Climate Change.

Verstegen, JA, Karssenberg, D, van der Hilst, F, Faaij, APC (2012) Spatio-temporal uncertainty in spatial decision support systems: a case study of changing land availability for bioenergy crops in Mozambique. Computers Environment and Urban Systems. 36, 30-42.

Wicke B, Verweij P, van Meijl H, van Vuuren DP and Faaij APC (2012) Indirect land use change: review of existing models and strategies for mitigation. Biofuels 3(1), 87-100.

Wicke, B., Sikkema, R., Dornburg, V., & Faaij, A. (2011). Exploring land use changes and the role of palm oil production in Indonesia and Malaysia. Land Use Policy, 193-206.

Wiens, J., Fargione, J., & Hill, J. (2011). Biofuels and biodiversity. Ecological Applications, 21, 1085-1095.

Wise, M., Hodson, E., Mignone, B., Clarke, L., Waldhoff, S., & Luckow, P. (2015). An approach to computing marginal land use change carbon intensities from bioenergy in policy applications. Energy Economics, 47, 307-318.

9 Appendices

Appendix 1 - Land-use classes in the natural vegetation case

Table 11: Land-use classes in the natural vegetation case

Class number	**Class name**
1	Ice
2	Tundra
3	Boreal forest
4	Cool conifer forest
5	Temperate mixed forest
6	Temperate deciduous forest
7	Warm mixed forest
8	Grassland/steppe
9	Hot desert
10	Shrubland
11	Savanna
12	Tropical woodland
13	Tropical forest

Appendix 2 - IMAGE regions map

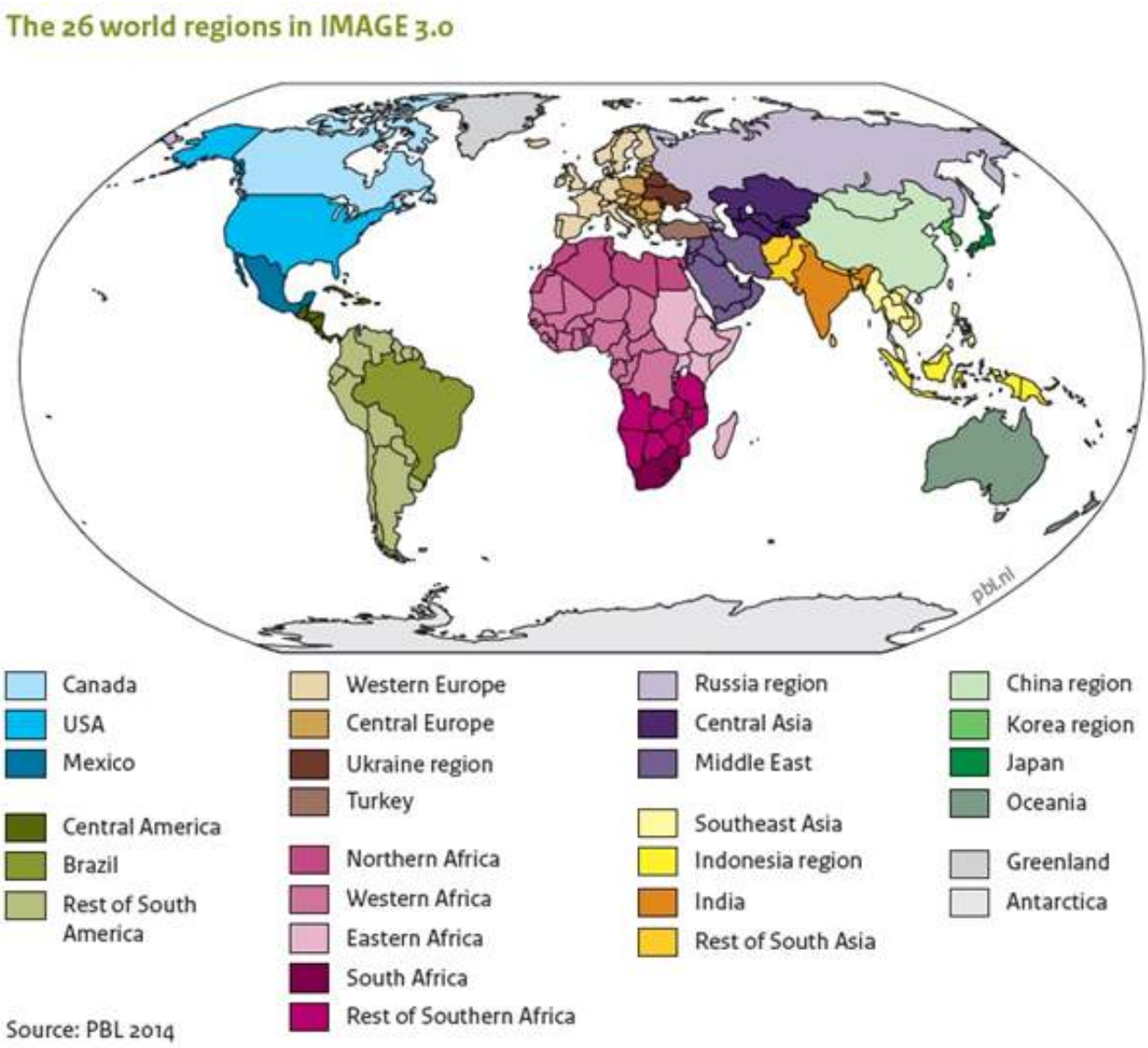

Figure 14: IMAGE regions map

Acknowledgements

Many thanks to the IMAGE representatives who entrusted me with using their data, which represents the basis for this thesis project. Special thanks to MSc. Vassilis Daioglou, Dr. Birka Wike, Dr. Floor van der Hilst, and MSc. Bala Bhavya Kausika for their input, feedback and support in carrying out the assessment.